(2)

THE CROSSFLOW SEPARATION OF A SUBMARINE CONFIGURATION IN A TURNING MANEUVER

by

Todd G. Wetzel and Roger L. Simpson
Department of Aerospace and Ocean Engineering
Virginia Polytechnic and State University
Blacksburg, VA

Report VPI-AOE-203

August 1993

REPORT DOCUMENTATION PAGE

Form Approved
OMB No. 0704-0188

1. AGENCY USE ONLY (Leave blank)	2. REPORT DATE	3. REPORT TYPE AND DATES COVERED
	9/1/93	Technical (5/91 - 9/93)

4. TITLE AND SUBTITLE
The Crossflow Separation of a Submarine Configuration in a Turning Maneuver

5. FUNDING NUMBERS
N00014-91-J-1732

6. AUTHOR(S)
Todd G. Wetzel and Roger L. Simpson

7. PERFORMING ORGANIZATION NAME(S) AND ADDRESS(ES)
Advanced Research Projects Agency, 3701 Fairfax Dr. Suite 100, Arlington, VA 22203-1714; through the Office of Naval Research, Applied Hydrodynamics, 800 N. Quincy St., Arlington, VA 22217

8. PERFORMING ORGANIZATION REPORT NUMBER
VPI-AOE-203

9. SPONSORING/MONITORING AGENCY NAME(S) AND ADDRESS(ES)

10. SPONSORING/MONITORING AGENCY REPORT NUMBER

11. SUPPLEMENTARY NOTES

12a. DISTRIBUTION/AVAILABILITY STATEMENT
Approved for Public Release, Distribution Unlimited.

12b. DISTRIBUTION CODE

13. ABSTRACT *(Maximum 200 words)*

The crossflow separation on a submarine configuration was studied. Forces and moments were taken for the submarine body alone, the body plus the sail, the body plus tail appendages, and the body with both a sail and tail appendages. Forces and moments wer taken at sideslip angles from 0° to 15°. Oil flows were done for the body alone for sideslip angles of up to 20°.

14. SUBJECT TERMS
Boundary Layer
Three Dimensional Separation
Control
Turbulence

15. NUMBER OF PAGES
43

16. PRICE CODE

17. SECURITY CLASSIFICATION OF REPORT	18. SECURITY CLASSIFICATION OF THIS PAGE	19. SECURITY CLASSIFICATION OF ABSTRACT	20. LIMITATION OF ABSTRACT
UNCLASSIFIED	UNCLASSIFIED	UNCLASSIFIED	

GENERAL INSTRUCTIONS FOR COMPLETING SF 298

The Report Documentation Page (RDP) is used in announcing and cataloging reports. It is important that this information be consistent with the rest of the report, particularly the cover and title page. Instructions for filling in each block of the form follow. It is important to ***stay within the lines*** to meet ***optical scanning requirements***.

Block 1. Agency Use Only *(Leave blank)*.

Block 2. Report Date. Full publication date including day, month, and year, if available (e.g. 1 Jan 88). Must cite at least the year.

Block 3. Type of Report and Dates Covered. State whether report is interim, final, etc. If applicable, enter inclusive report dates (e.g. 10 Jun 87 - 30 Jun 88).

Block 4. Title and Subtitle. A title is taken from the part of the report that provides the most meaningful and complete information. When a report is prepared in more than one volume, repeat the primary title, add volume number, and include subtitle for the specific volume. On classified documents enter the title classification in parentheses.

Block 5. Funding Numbers. To include contract and grant numbers; may include program element number(s), project number(s), task number(s), and work unit number(s). Use the following labels:

C	- Contract	**PR**	- Project
G	- Grant	**TA**	- Task
PE	- Program Element	**WU**	- Work Unit Accession No

Block 6. Author(s). Name(s) of person(s) responsible for writing the report, performing the research, or credited with the content of the report. If editor or compiler, this should follow the name(s).

Block 7. Performing Organization Name(s) and Address(es). Self-explanatory.

Block 8. Performing Organization Report Number. Enter the unique alphanumeric report number(s) assigned by the organization performing the report.

Block 9. Sponsoring/Monitoring Agency Name(s) and Address(es). Self-explanatory.

Block 10. Sponsoring/Monitoring Agency Report Number. ***(If known)***

Block 11. Supplementary Notes. Enter information not included elsewhere such as: Prepared in cooperation with...; Trans. of...; To be published in.... When a report is revised, include a statement whether the new report supersedes or supplements the older report.

Block 12a. Distribution/Availability Statement. Denotes public availability or limitations. Cite any availability to the public. Enter additional limitations or special markings in all capitals (e.g. NOFORN, REL, ITAR).

- **DOD** - See DoDD 5230.24, "Distribution Statements on Technical Documents."
- **DOE** - See authorities.
- **NASA** - See Handbook NHB 2200.2.
- **NTIS** - Leave blank.

Block 12b. Distribution Code.

- **DOD** - Leave blank.
- **DOE** - Enter DOE distribution categories from the Standard Distribution for Unclassified Scientific and Technical Reports.
- **NASA** - Leave blank.
- **NTIS** - Leave blank

Block 13. Abstract. Include a brief *(Maximum 200 words)* factual summary of the most significant information contained in the report.

Block 14. Subject Terms. Keywords or phrases identifying major subjects in the report.

Block 15. Number of Pages. Enter the total number of pages.

Block 16. Price Code. Enter appropriate price code *(NTIS only)*.

Blocks 17. - 19. Security Classifications. Self-explanatory. Enter U.S. Security Classification in accordance with U.S. Security Regulations (i.e., UNCLASSIFIED). If form contains classified information, stamp classification on the top and bottom of the page.

Block 20. Limitation of Abstract. This block must be completed to assign a limitation to the abstract. Enter either UL (unlimited) or SAR (same as report). An entry in this block is necessary if the abstract is to be limited. If blank, the abstract is assumed to be unlimited.

DISCLAIMER NOTICE

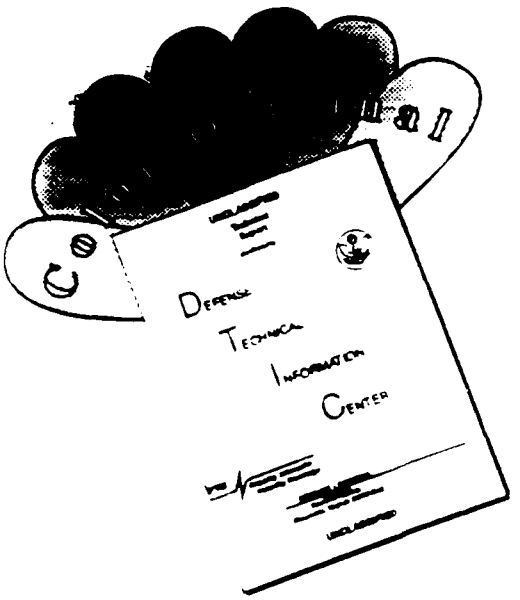

THIS DOCUMENT IS BEST QUALITY AVAILABLE. THE COPY FURNISHED TO DTIC CONTAINED A SIGNIFICANT NUMBER OF COLOR PAGES WHICH DO NOT REPRODUCE LEGIBLY ON BLACK AND WHITE MICROFICHE.

Abstract

The crossflow separation on a submarine configuration was studied. Forces and moments were taken for the submarine body alone, the body plus the sail, the body plus tail appendages, and the body with both a sail and tail appendages. Forces and moments were taken at sideslip angles from 0° to 15°. Oil flows were done for the body alone at sideslip angles of up to 20°.

Nomenclature

bte	fin trailing edge span
c	submarine chord (length)
cr	fin root chord
ct	fin tip chord
C_l	roll moment coefficient, body axes, L/qc^3
C_m	pitching moment coefficient, body axes, M/qc^3
C_n	yaw moment coefficient, body axes, N/qc^3
C_x	axial force coefficient, body axes, X/qc^2
C_y	normal or side force coefficient, body axes, Y/qc^2
C_z	vertical force coefficient, body axes, Z/qc^2
d	submarine diameter
D_h	horizontal diameter (submarine width)
D_v	vertical diameter (submarine height)
L	roll moment, body axes
M	pitching moment, body axes
N	yaw moment, body axes
p	free-stream pressure
q	dynamic pressure, $(1/2)\rho U_\infty^2$
Re	chord Reynolds number, $\rho U_\infty c/\mu$

R_1	primary reattachment
R_2	secondary reattachment
S_{ref}	reference area
S_1	primary separation
S_2	secondary separation
tr	fin root thickness
U_∞	free-stream velocity
x	longitudinal distance along submarine from nose
xr	fin chord ordinate, referenced from trailing edge
X	axial force, body axes
Y	normal or side force, body axes
Z	vertical force, body axes
β	sideslip angle,
o	angular location around cross section measured from windward side
ρ	fluid density

Introduction

Turning maneuvers of submarines result in crossflow separation that generates large hydrodynamic forces and moments that substantially oppose the maneuver. The separation of a simple axisymmetric body is very complex in nature. The addition of appendages, such as a sail and tail control surfaces in the case of the submarine, further complicates the flow field and submarine design. Understanding these flow field interactions is paramount to improving vehicle performance and design capabilities. Presently, computational methods slowly continue to improve the designer's ability to

account for these complexities. However, much experimental data is still needed in order to guide further computational developments. Such data is presented herein.

The data presented in this report supplements the data found in Wetzel and Simpson (1992a, 1992b, 1993) and Wetzel, Simpson, and Liapis (1993).

Previous Research

Axisymmetric bodies yawed to the freestream flow, like submarines in a turning maneuver, produce large amounts of vortical separation. Bushnell and Donaldson (1990) note that vortical flow affects acoustic and non-acoustic stealth, propulsion efficiency and body drag, control effectiveness, and maneuverability. The focus of this report is on maneuverability.

This separation is dominated by the crossflow component of the flow velocity. Figure 1 shows typical flow structures in such a crossflow separation (Ahn and Simpson, 1992). For circular cylindrical bodies at 15° sideslip, the crossflow usually separates near $\phi = 105°$ (Poll, 1985).

These flows are highly sensitive to Reynolds number effects (Bushnell and Donaldson 1990). Ahn and Simpson (1992) have studied the vortical flow on a prolate spheroid at angle of attack, which is similar to the submarine at yaw. In such a case, the primary separation location is largely dependent on the state of the boundary layer (laminar, transitional, or turbulent), which is a function of Reynolds number (Ahn and Simpson, 1992). For high Reynolds number flows or flows with boundary layer transition fixed such that the boundary layer is turbulent at separation, Ahn shows that the separation line dependency on Reynolds number is greatly reduced. The separation line no longer changes much circumferentially, but gradually extends upstream on the body with an increase in Reynolds number (Ahn and Simpson, 1992)

Ahn also studied the effects of angle of attack on the primary separation line. At increasing angle of attack, the separation line moves farther towards the leeside and farther upstream on the body (Ahn and Simpson, 1992).

Wetzel and Simpson (1992a, 1992b, 1993) and Wetzel, Simpson, and Liapis (1993) have extended these studies to a submarine-like configuration. The crossflow separation was studied on a 688 class submarine in a sideslip and many of the same flow features described by Ahn and Simpson were found. At a Reynolds number of 6.8 million with the boundary layer tripped, both primary and secondary separation lines were observed at 15° sideslip. In addition, the separation off the sail was found to greatly influence the flow field. This sail separation forced the separation line immediately aft of the sail to be located at the sail trailing edge, regardless of angle of sideslip. This in turn was found to introduce relatively large out-of-plane forces and moments. Wetzel and Simpson (1992a, 1992b, 1993) and Wetzel, Simpson, and Liapis (1993) also showed that vortex generators could be used very effectively to control this separation.

Experimental Apparatus

The Wind Tunnel

All tests were performed in the VPI&SU Stability Wind Tunnel. This continuous, closed return, subsonic wind tunnel has a 25 ft. long, 6 x 6 ft. square interchangeable test section. The tunnel has a flow speed range of 0-220 ft/s and a maximum unit Reynolds number of 1.33×10^6 per foot. The tunnel is powered by a 600 hp DC motor which turns a 14 ft diameter prop. The flow is directed through screens and a 9:1 contraction with a very low-turbulence intensity of around 0.03%. The tunnel allows force and moment measurements to be taken from either a strut or sting mounted strain gauge balance. The sting was selected for its lower interference with the flow and its higher ranges of force and moment measurements.

The Submarine Model

A 1/48 scale Los Angeles class (688) submarine model (Scale Shipyard, 1991) was built (Figure 2). The model is nominally 90.25" long and has a nominal 8.25" maximum diameter. The model structure consists of a fiberglass skin mated to an aluminum skeleton. The propeller was not modeled, but rear control surfaces were modeled. The towed array housing, sail diving planes and sail were all modeled. The black body surface was marked with a white grid spaced every 4" in the longitudinal direction and every 45° in the circumferential direction. When the model was in the tunnel, all mounting holes were filled with red vacuum wax and/or plaster.

To trip the flow, posts 21 mils high, 0.1" center to center, and 0.05" in diameter were placed around the nose at x/c=0.044 and along the length of the model at +/-45° from the windward side of the model to act as trip strips (Smith, 1989). The trip strips were placed on the nose to guarantee tripped boundary layers at low angles of sideslip, while the longitudinal trips were effective for higher angles of sideslip. The trip strips were also placed on the sail and all control surfaces. Previous tests (Wetzel and Simpson, 1992, 1993) indicated little Re dependence from Re = 4.6 million to 8.8 million, so the trip strips were effective.

To simulate a turning maneuver, the model was placed in a sideslip. The model was mounted in the tunnel on its side in order to utilize the adjustable angle of attack feature of the strut-mounted sting (Figure 3). The towed array was placed on the windward side, so a left turn was modeled. Sideslip angles of up to 15° were simulated. For the various force and moments test, the various submarine components (sail, tail appendages) were systematically removed in order to test the aerodynamic dependence on the configuration (Figure 4).

Instrumentation and Experimental Techniques

Forces and Moments

A six-component strain gauge balance made by the Transducer Systems Division of Modern Machine and Tool, Inc., of Newport News, Virginia, was used for the force and moment measurements. All data were collected with a Hewlett-Packard Model 3052 data acquisition unit. Each reading was the average of 50 values. The data are reported in body axes with the moments taken about the quarter chord of the sail (Figure 5). Runs were made for wind tunnel speeds of 150 ft/s (Reynolds number of 6.84 million) and at sideslip angles of 0 to 15°. The uncertainties were estimated at 20:1 odds to be δC_x=+/-0.0002, δC_y=+/-0.0004, δC_z=+/-0.0005, δC_l=+/-0.00002, δC_m=+/-0.0001, and δC_n=+/-0.0002.

Oil Flows

A primary diagnostic for these tests was surface oil flow visualization. The oil flow mixture consisted of titanium dioxide (TiO_2) as a pigment, kerosene for the solvent, and oleic acid to prevent coagulation or lumping of the TiO_2. The mixture is made by adding 40 ml of sifted, unpacked TiO_2 to a 100 ml graduated cylinder. Kerosene is added up to the 100 ml mark, and 5 ml of Oleic acid is added on top of that. Several variations of this mixture were tried during the first couple runs, and the quality of the runs was found to be relatively insensitive to small changes from this recipe. The mixtures are then thoroughly stirred and transferred to a pail. A sponge brush is used to apply a coat of the mixture to the model. Brush strokes are made normal to the expected flow direction so that brush marks are not later misinterpreted as skin friction lines.

After the tunnel is turned on and the oil mixture is almost entirely dry, the tunnel is turned off. The oil flows are recorded by photographing the model in sections and from different peripheral orientations. Also, separation locations are directly measured off the

model surface and recorded. After carefully recording the flow separation location, the dried mixture is then cleaned off with kerosene.

Lines of separation are indicated by converging surface skin friction line patterns. The peripheral angle separation location ϕ is measured from the windward side, counter-clockwise facing the model (Figure 1). The indicated ϕ is probably premature for two reasons. The oil flow mixture is drawn down (towards the windward side) due to gravitational effects, and the oil flow mixture itself initiates separation earlier then would occur on a clean surface. Simpson et. al. (1992) have shown that these effects can add errors of up to -5° for a similar flow at 30° angle of attack to the free-stream flow. No attempts were made to correct any of the present data. The locations were measured by placing a flexible ruler on the model surface and measuring the separation location relative to a grid line. This measurement technique has an uncertainty of +/- 1°. It is estimated that uncertainties due to the sometimes subjective nature of exactly selecting the separation location in a difficult to read oil flow is on the order of +/-2°.

It can be very difficult to determine exactly the streamwise location where separation begins. Separation lines are located at converging skin friction lines in the oil flow pattern. Simpson et al. (1992) have proposed, as a rule of thumb, that the point where the angle of incidence of converging skin friction lines is smallest but positive be interpreted as the start of open separation. Downstream of this location the skin friction lines on each side of the separation line intersect the separation line at a sharp finite angle.

Experimental Results

Forces and Moments

Figure 6 shows the variations of the forces and moments with sideslip angle for the body alone, the body plus sail, the body plus tail, and the body plus sail and tail. The in-plane forces and moments (C_x, C_y and C_n) are the ones directly affected the sideslip angle. The side force C_y and yaw moment C_n both vary relatively linearly with sideslip

angle. The tail surprisingly has little effect on the yaw moment, but the sail increases the yaw moment slope significantly. The sail and tail together result in slightly lower C_n at high sideslip angles when compared to the body and sail combination.

The tail does significantly increase the side force C_y, and once again the sail has an even more pronounced effect. Together, the sail and tail combine for the highest side force.

The axial force plot is much less smooth. It is noted that the axial force is necessarily going to carry the largest errors due to the lack of a complete tail and sting interference. It is clear from the plots, however, that as expected adding the sail and tail increase the axial force.

The out-of-plane forces and moments also experience interesting trends. Both the vertical force C_z and the pitching moment C_m are practically zero for the body and body/tail configurations. However, the addition of the sail results in significant vertical force and pitching moment at high sideslip angles. The roll moment is also relatively small for the body and body/tail configurations, but the addition of the sail results in a negative roll component. In addition, the sail and tail combined result in very complex roll interactions.

Oil Flows

Oil flows were performed on the body alone at sideslip angles from 5° to 20°. Photographs of these oil flows can be found in Appendix I. At 5°, no separation was clear enough to record. Figure 7, however, shows the primary separation lines for the body at 10° sideslip. It is important to note that the body alone was not purely symmetrical as the top of the model still had the towed array housing. Therefore, the separation lines for the top and bottom of the submarine should be expected to be slightly different. At 10° sideslip the flow separates at about 130° near the nose and closer to 95° near the tail. Figure 8 (Wetzel, Simpson and Liapis, 1993) shows previously taken data for the body

with the sail. It is clear that the separation line on the sail side is much closer to 90° immediately aft of the sail but climbs as high as 135° for much of the length of the body.

At 15° sideslip (Figure 9) there is also a secondary separation line at about 150°. The primary separation line occurs several degrees sooner at 15° sideslip than it does at 10°. Once again, Figure 10 shows presiously taken data for the body with the sail, and the primary separation line on the sail side is just past ϕ=90° immediately aft of the sail. This primary separation line eventually climbs to ϕ=110° farther downstream of the sail. At 20° sideslip (Figure 10), the flow is again very similar to the flow at 15° sideslip.

Conclusions

The effect of submarine configuration on the aerodynamic forces and moments was studied. It was found that the sail affects the in-plane forces and moments more than the tail appendages do. It was also found that the sail introduces significant out-of-plane forces and moments.

Oil flows were performed on the body alone. Separation was hard to distinguish at 5° sideslip, but primary separation lines were located at 10° sideslip. At both 15° and 20° sideslip, both primary and secondary separation lines were located. As expected, the separation lines moved towards the windward side as sideslip angle was increased.

Acknowledgments

This work was supported by the National Science Foundation through a Graduate Fellowship and the Defense Advanced Research Projects Agency (Gary W. Jones, Program Manager) through the Office of Naval Research Grant N00014-91-J-1732 (James A. Fein, Program Manager).

References

Ahn, S. and Simpson, R.L., 1992: *Cross-Flow Separation on a Prolate Spheroid at Angles of Attack*, AIAA-92-0428.

Bushnell, D.M., and Donaldson, C.D., 1990: *Control of Submersible Vortex Flows*, NASA Technical Memorandum no. 102693.

Poll, D.I.A., 1985: "On the Effect of Boundary Layer Transition on a Cylindrical Afterbody at Incidence in Low-speed Flow", *Aero J.*, pp. 315-327.

The Scale Shipyard, 5866 Orange Ave. #3, Long Beach, CA 90805-4146.

Smith, D. G.,1989: *Private Communication*, Aerodynamics Laboratory, Boeing Commercial Airplanes.

Simpson, R. L., Walker, D.A., and Shinpaugh, K.A., 1992: *Description of a 1000 Sensor Constant Current Anemometer System for Locating Three-Dimensional Turbulent Boundary Layer Separations*, Report VPI-AOE-185, distributed by DTIC for Defense Advanced Research Projects Agency.

Wetzel, T.G. and Simpson, R.L., 1992(a): *The Effect of Vortex Generators on Crossflow Separation on a Submarine in a Turning Maneuver*, Report VPI-AOE-186, distributed by DTIC for Defense Advanced Research Projects Agency.

Wetzel, T.G. and Simpson, R.L., 1992(b): "The Effect of Vortex Generators on Crossflow Separation on a Submarine in a Turning Maneuver", *Proceedings of the Fifth Submarine Technology Symposium*, Applied Physics Laboratory, Johns Hopkins University, Laurel, Maryland, pp. 185-198.

Wetzel, T.G. and Simpson, R.L., 1993: *The Effect of Vortex Generating Fins and Jets on Crossflow Separation on a Submarine in a Turning Maneuver*, 31st Aerospace Sciences Meeting and Exhibit, Reno, Nevada, AIAA 93-0862.

Wetzel, T.G., Simpson, R.L., and Liapis, S., 1993: *The Effect of Vortex Generating Fins and Jets on Crossflow Separation on a Submarine in a Turning Maneuver*, Report VPI-AOE-195, distributed by DTIC for Advanced Research Projects Agency.

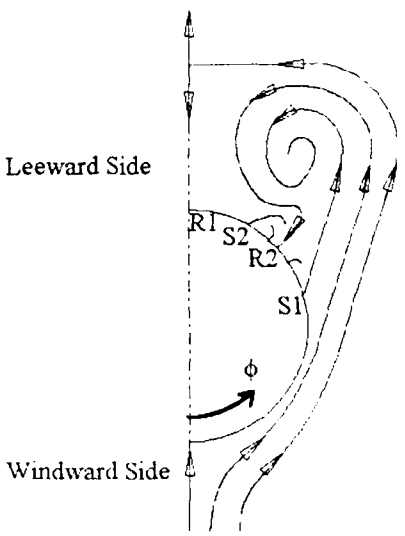

Figure 1. Crossflow separation (Ahn, 1992). This half-cross-section of the submarine shows the important flow phenomena. The addition of vortex generators delays separation (S1 and S2) farther around the leeward side of the submarine. Primary separation (S1) is the flow phenomenon discussed in this report.

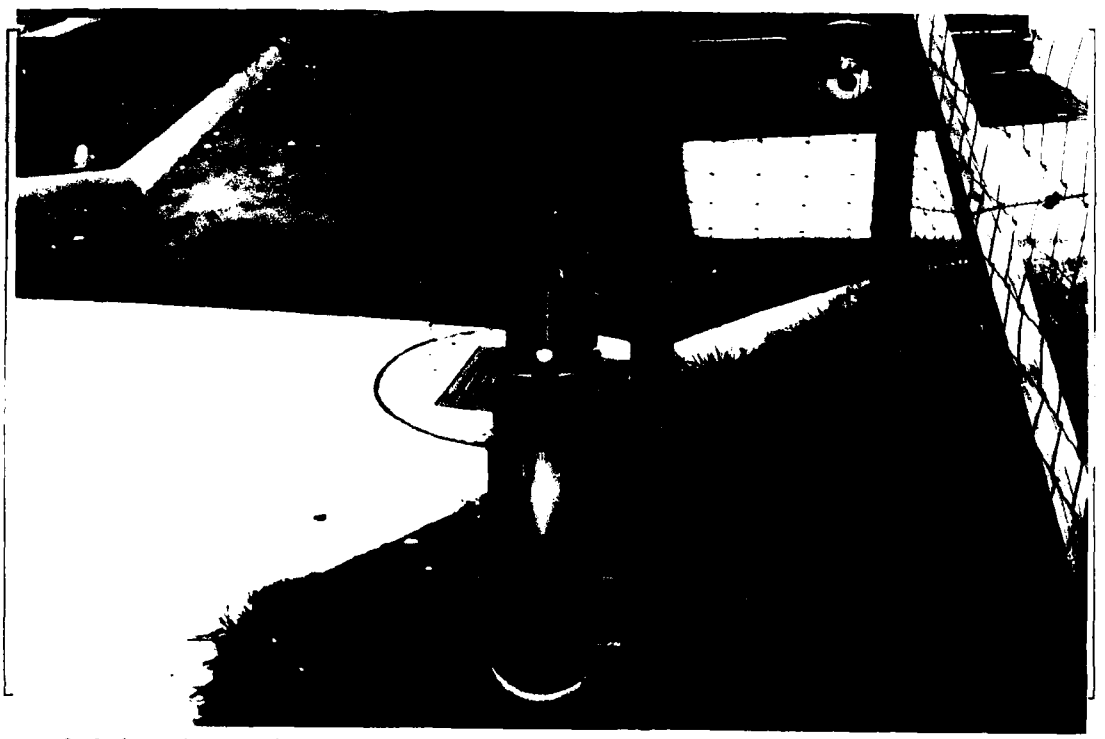

Figure 2. Submarine Model.

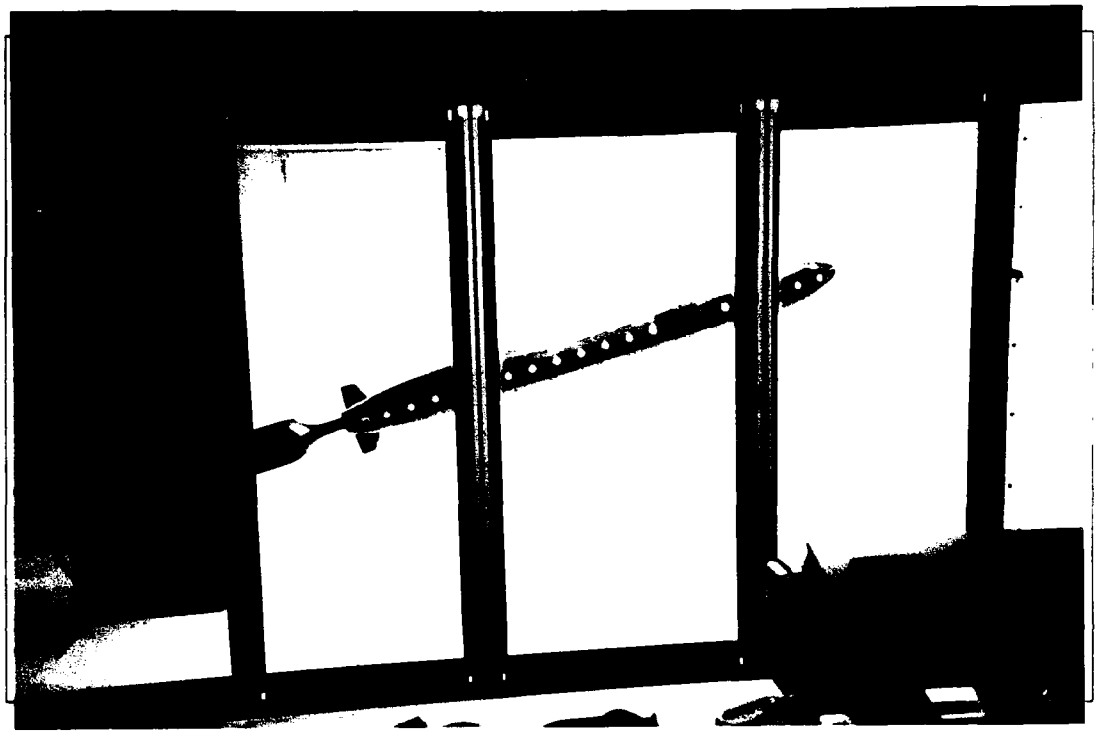

Figure 3. Model in the wind tunnel.

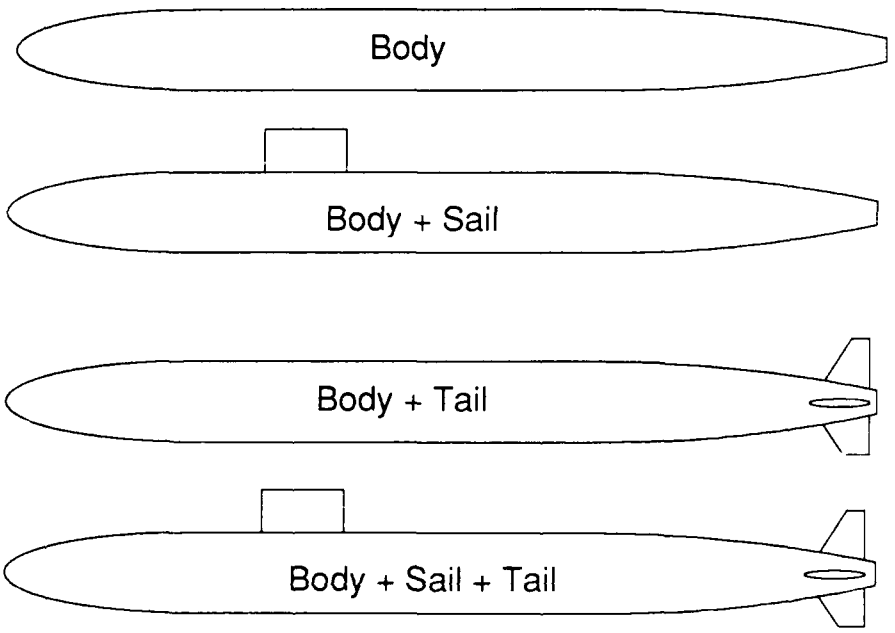

Figure 4. Model configurations.

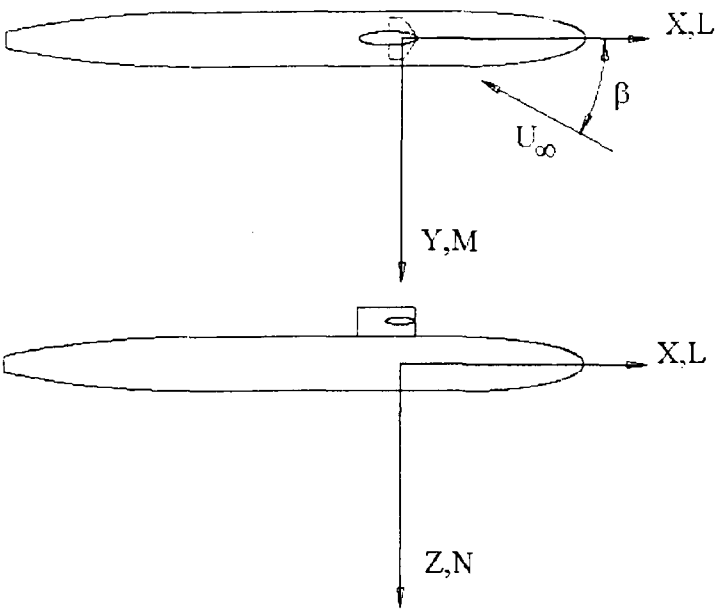

Figure 5. Body axes notation.

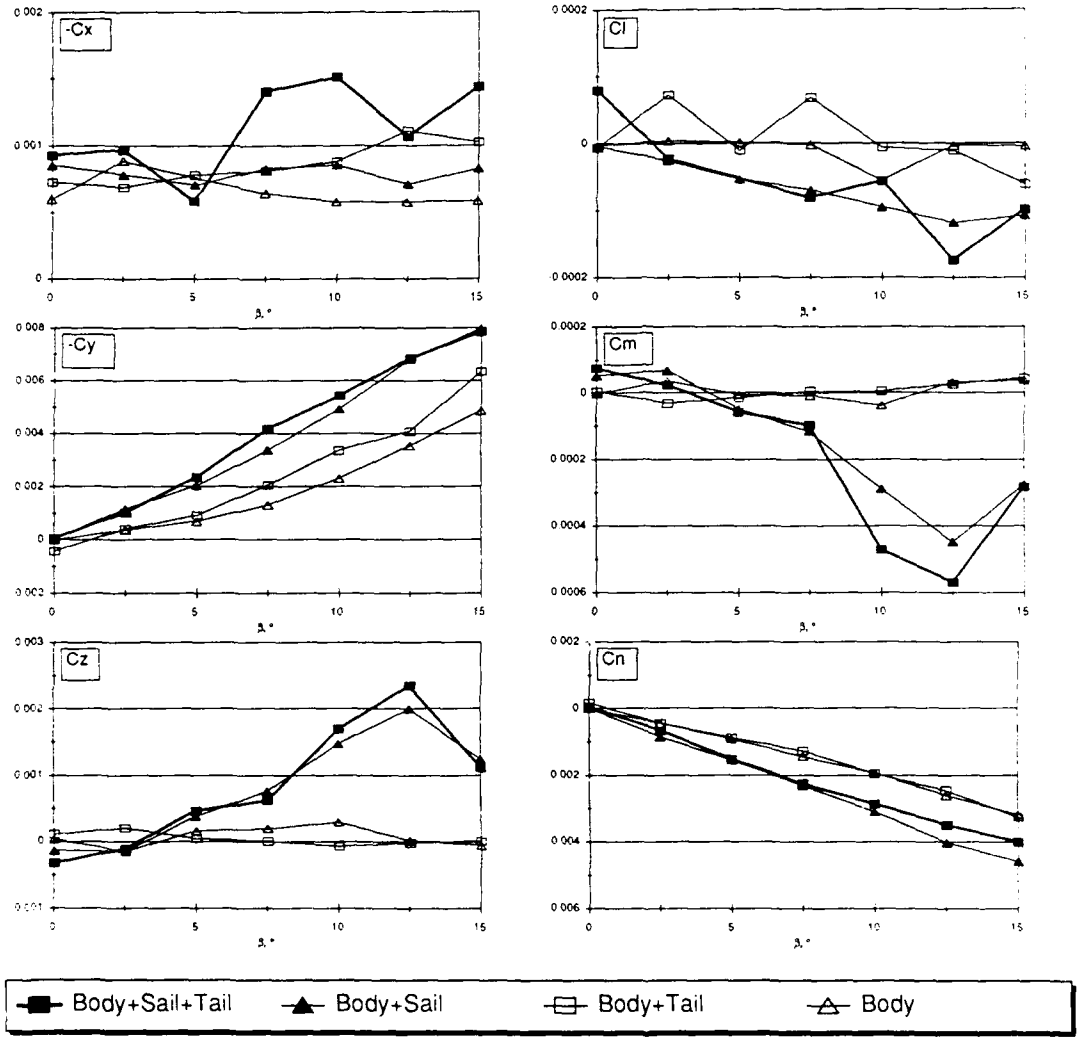

Figure 6. Forces and moments acting on different submarine configurations. Re = 6.8 million. Lines for visual aid only.

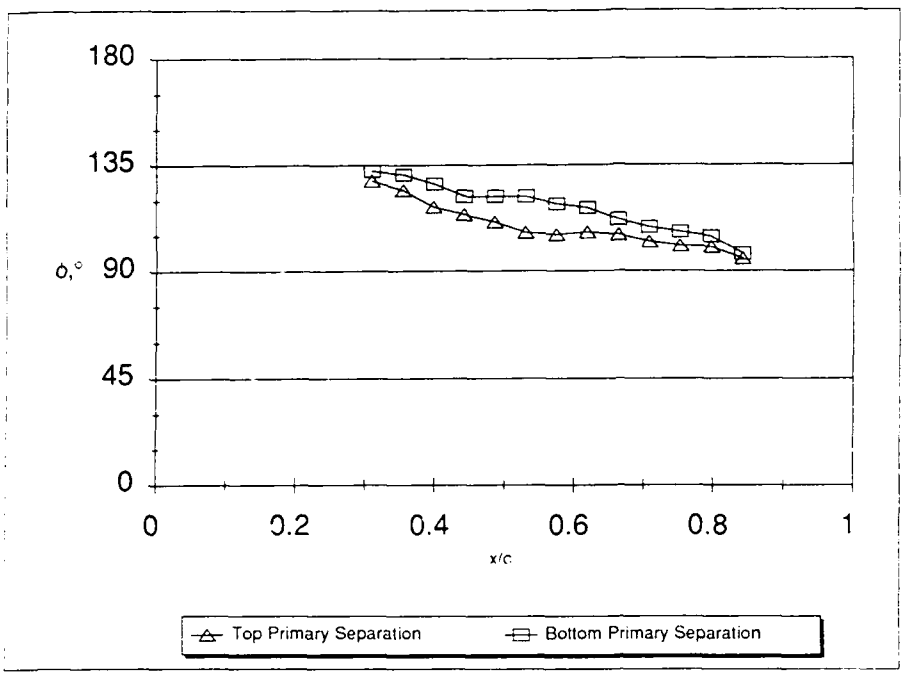

Figure 7. Primary separation lines for the model without appendages at 10° sideslip. Re = 6.8 million.

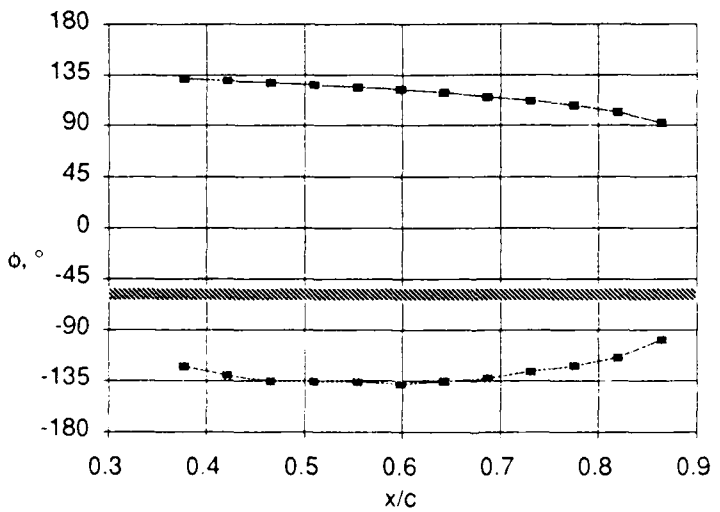

Figure 8. Separation line for body plus sail, Re = 6.8 million, β=10°. Shaded bar represents towed array housing. Taken from Wetzel, Simpson, and Liapis (1993).

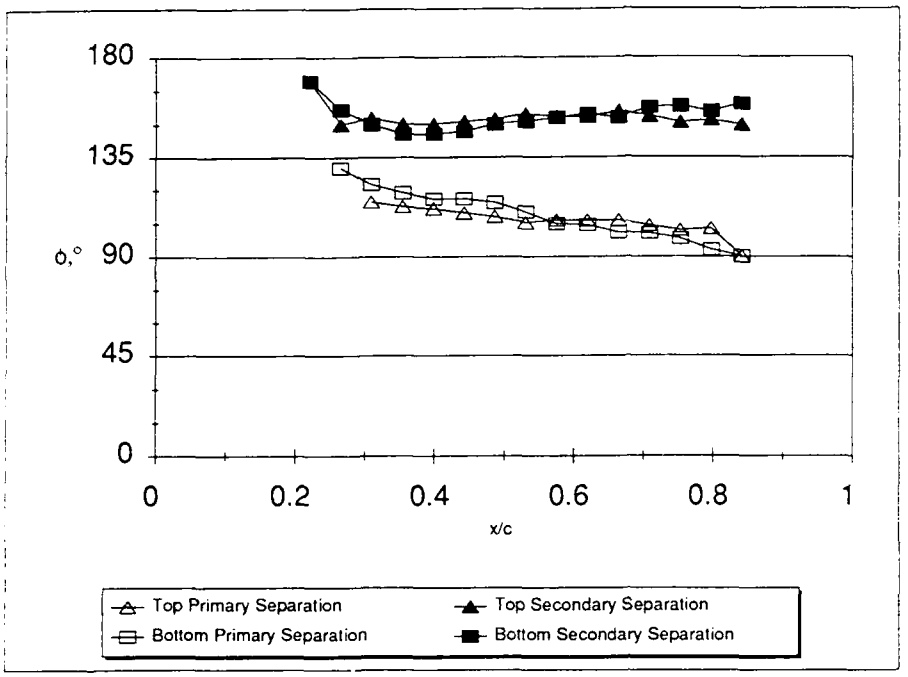

Figure 9. Primary and secondary separation lines for the model without appendages at 15° sideslip. Re = 6.8 million.

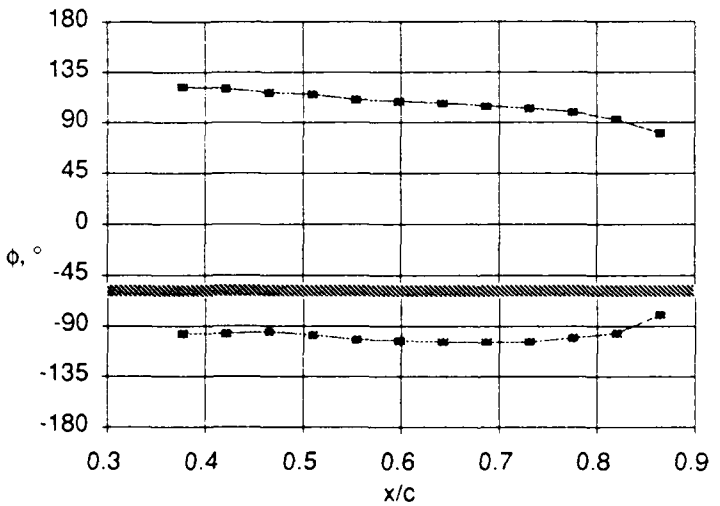

Figure 10. Separation line for body plus tail, Re =6.8 million, β=15°. Shaded bar represents towed array housing. Taken from Wetzel, Simpson, and Liapis (1993).

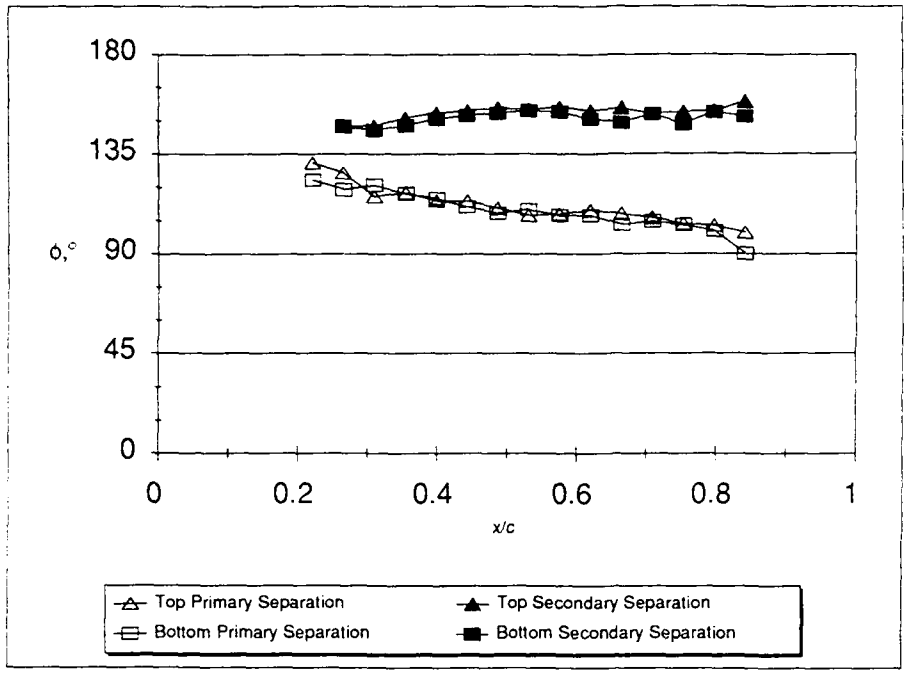

Figure 11. Primary and Secondary separation lines for the model without appendages at 20° sideslip.

Appendix I - Oil Flow Photographs

The following photographs document the oil flows performed in this study. The photographs were taken on each side of the leeward side at about 45° off vertical. All oil flows were done at a Reynolds number of 6.8 million. In this study, only the body and towed array housing were modeled. The tail appendages and sail were removed. The captions list the range in inches of the visible circumferential grid lines in each photo. The longitudinal gridline in the middle of each of the photographs correspods to ϕ = +/-135°.

ß=20°, Top of Submarine (with towed array housing).

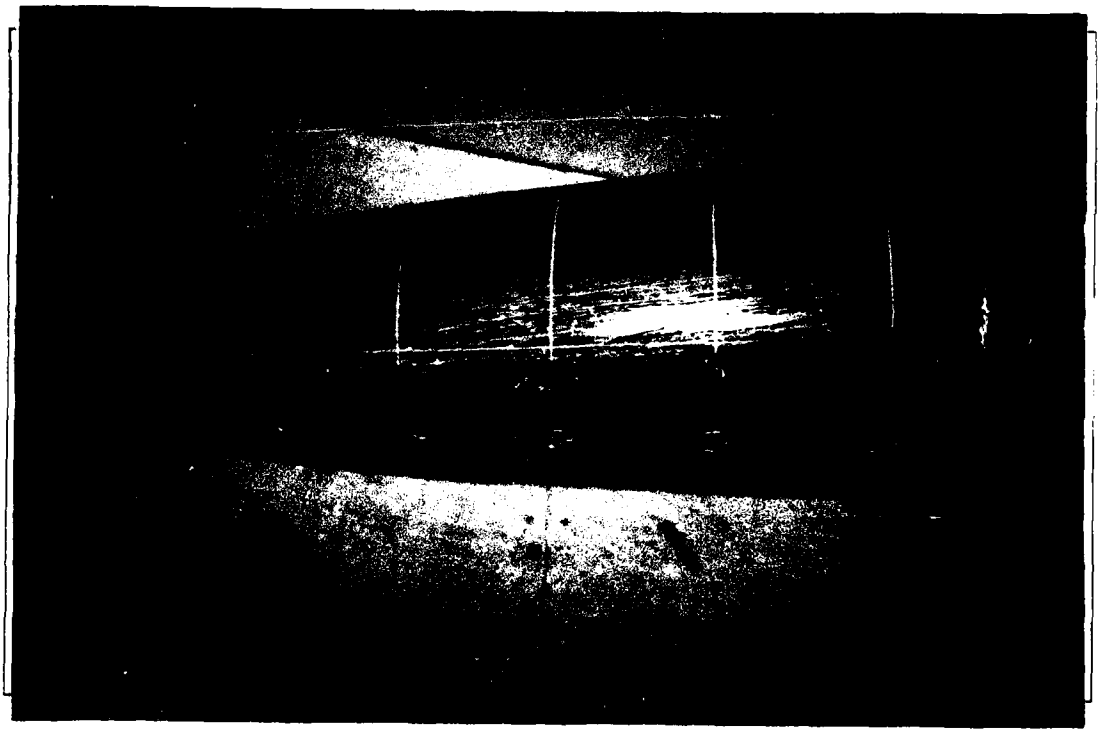

Figure A1. x = 56" to tail.

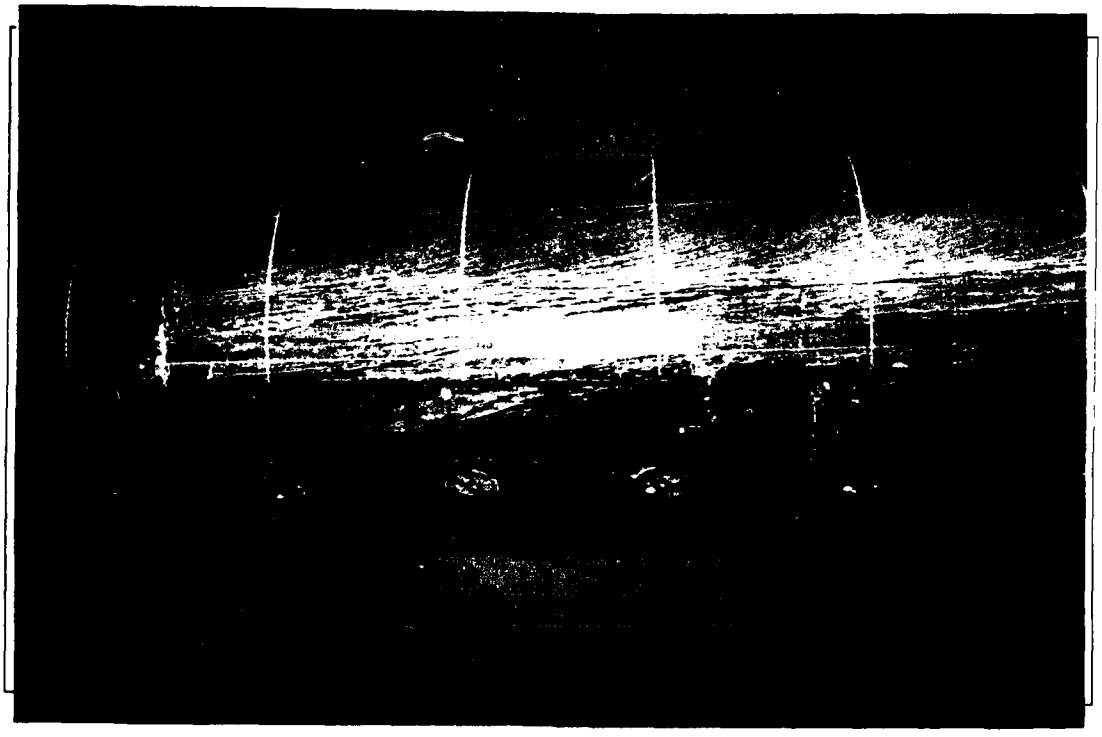

Figure A2. x = 40" to x = 60".

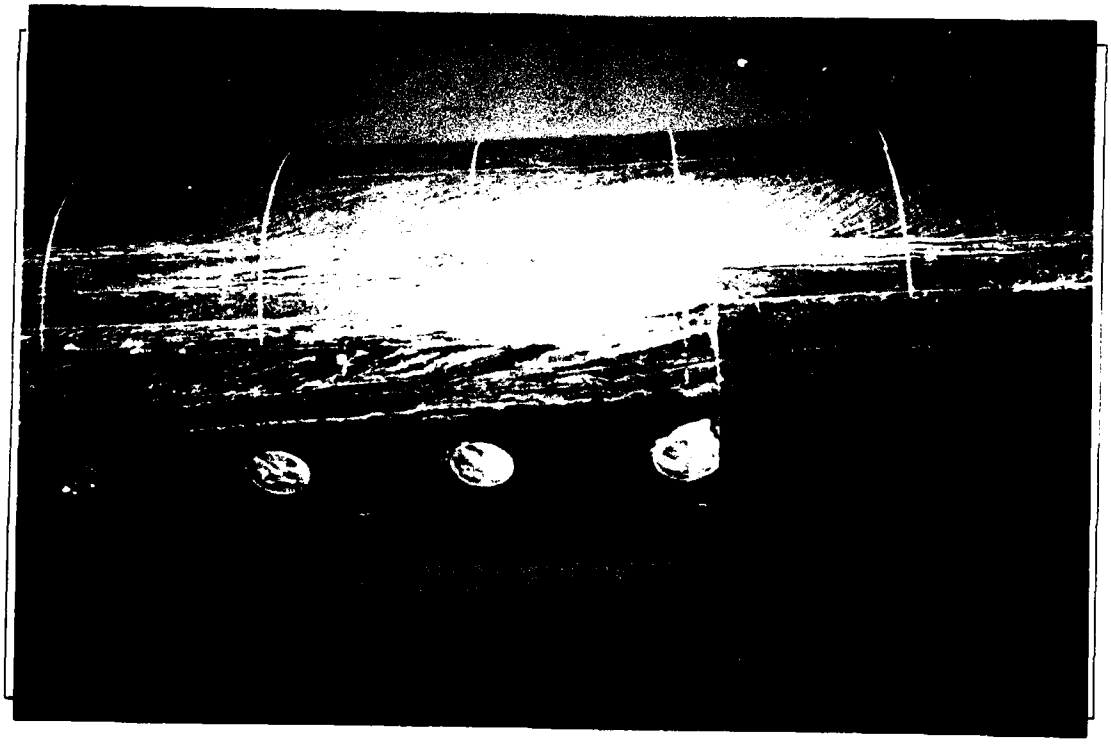

Figure A3. x = 28" to x = 44".

Figure A4. x = 16" to x = 32".

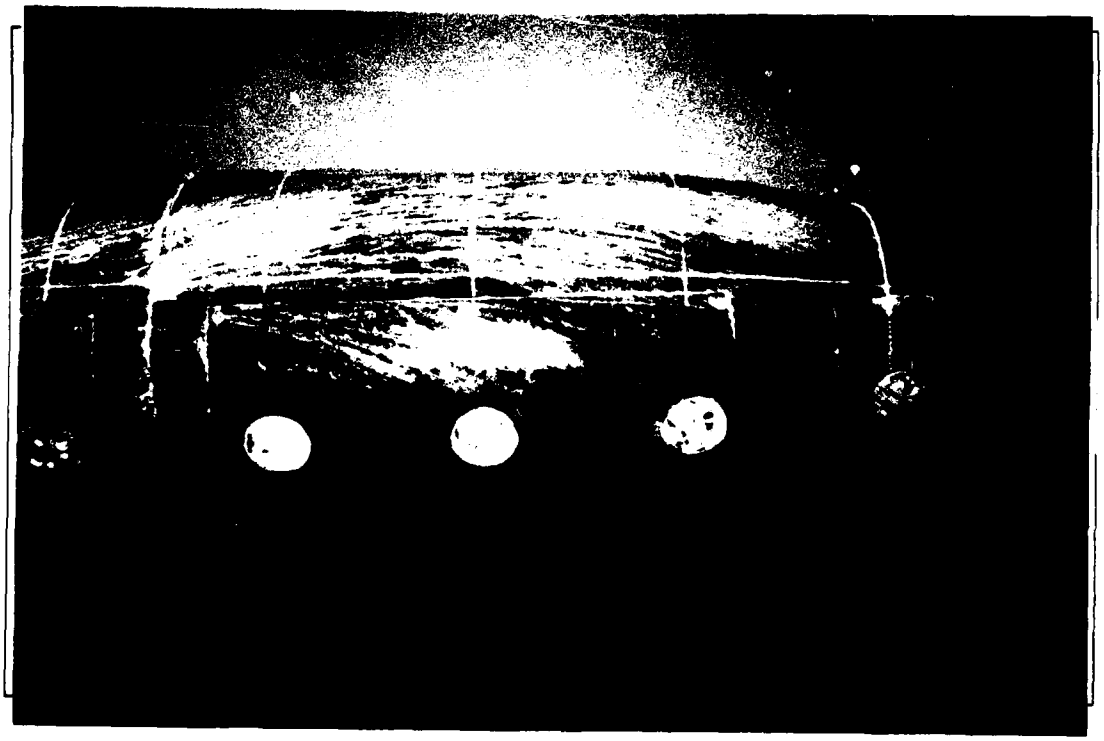

Figure A5. x = 0" to x = 20".

ß=20°, Bottom of Submarine.

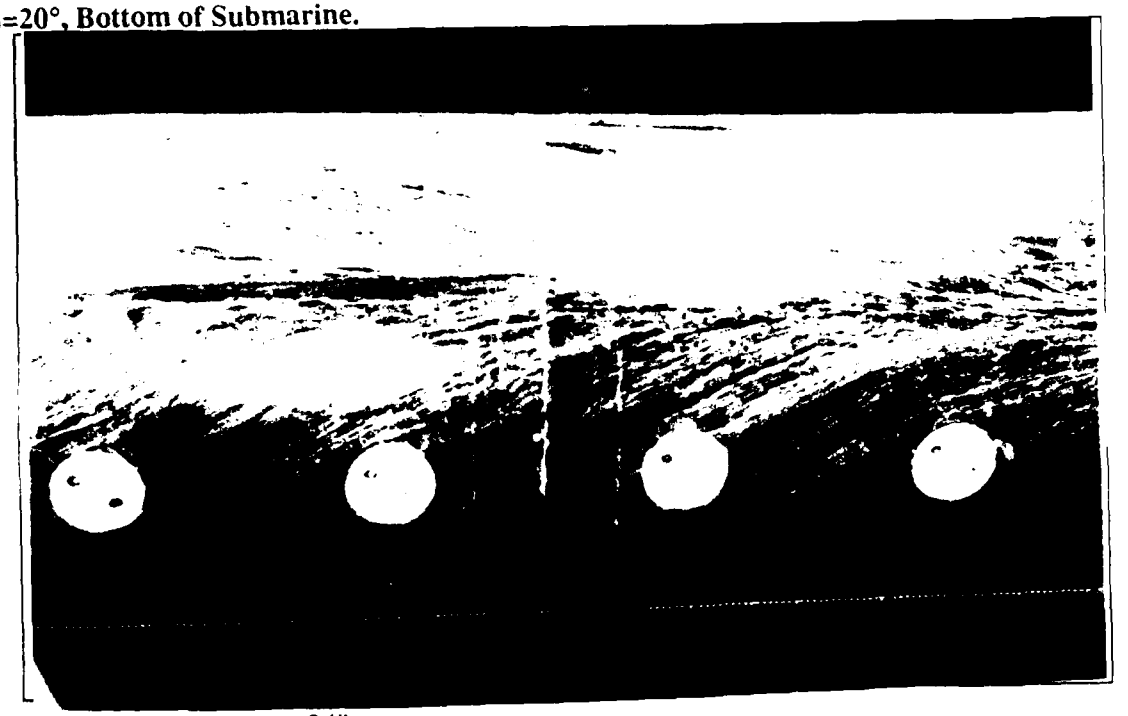

Figure A6. x = 12" to x = 24".

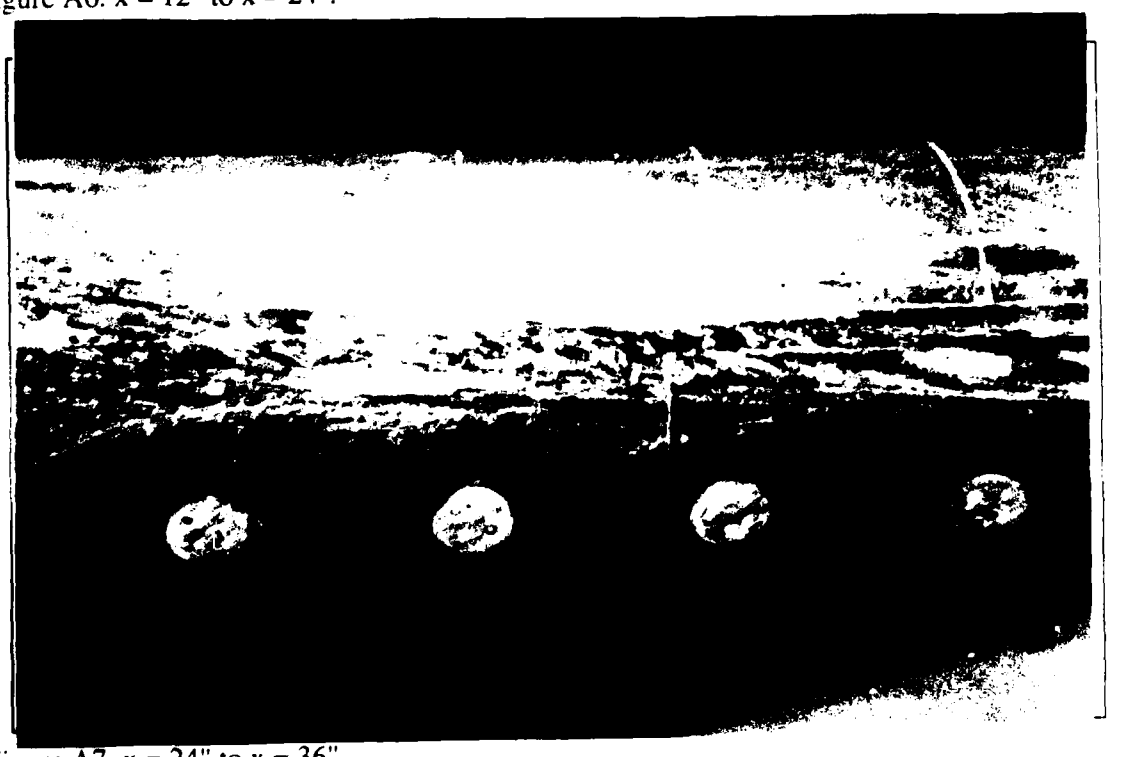

Figure A7. x = 24" to x = 36".

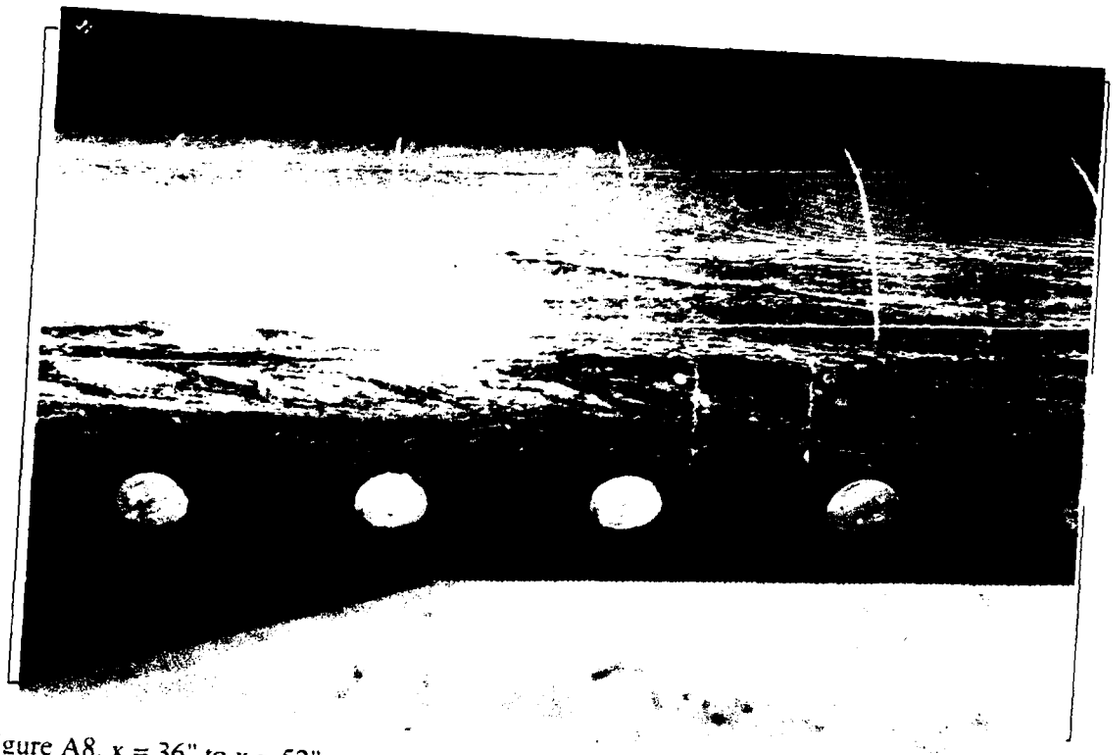

Figure A8. x = 36" to x = 52".

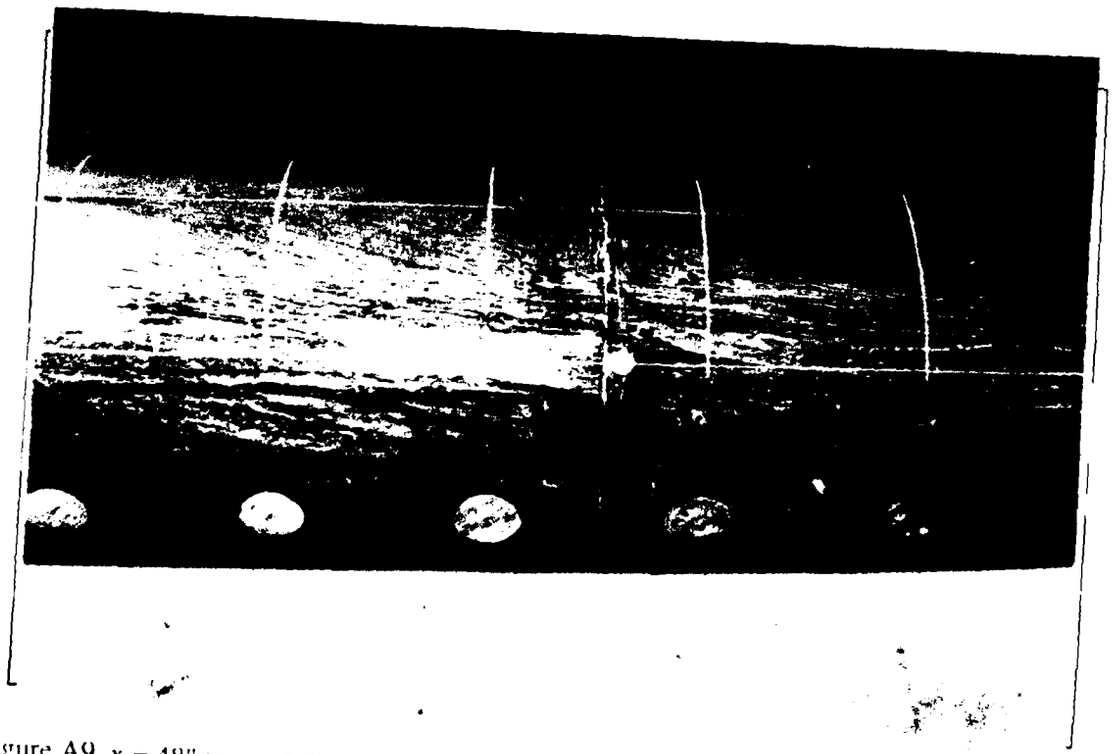

Figure A9. x = 48" to x = 64".

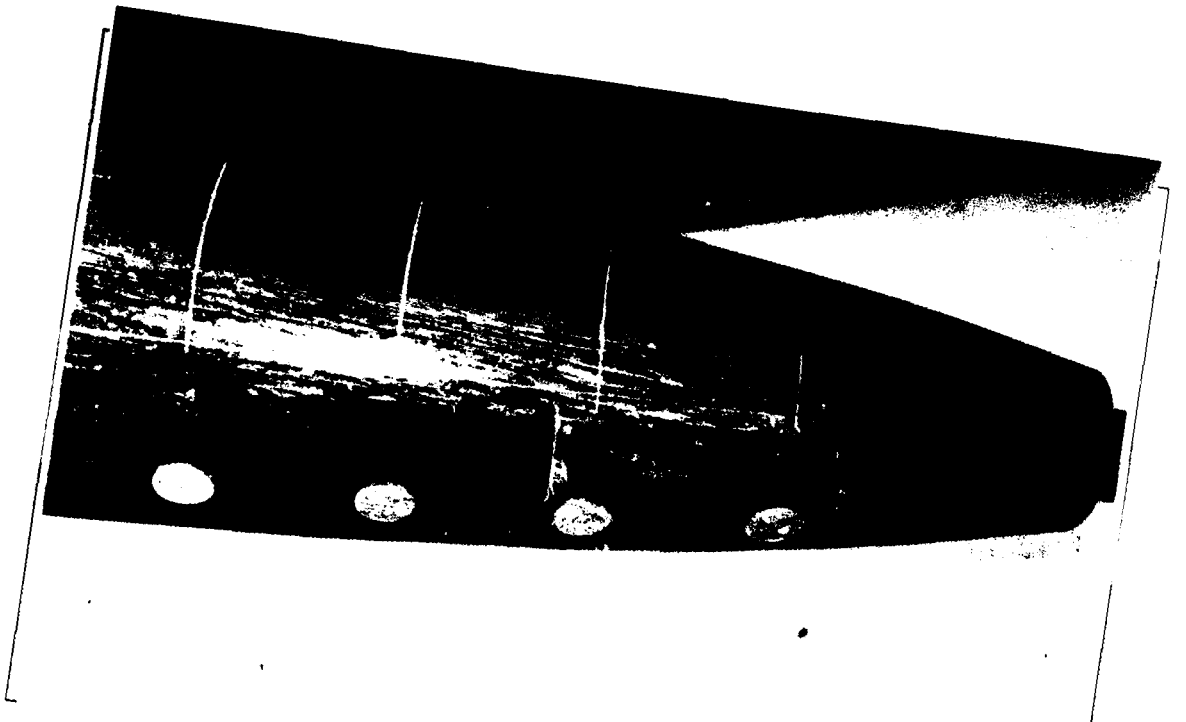

Figure A10. x = 64" to tail.

ß=15°, Top of Submarine (with towed array housing).

Figure A11. x = 60" to tail.

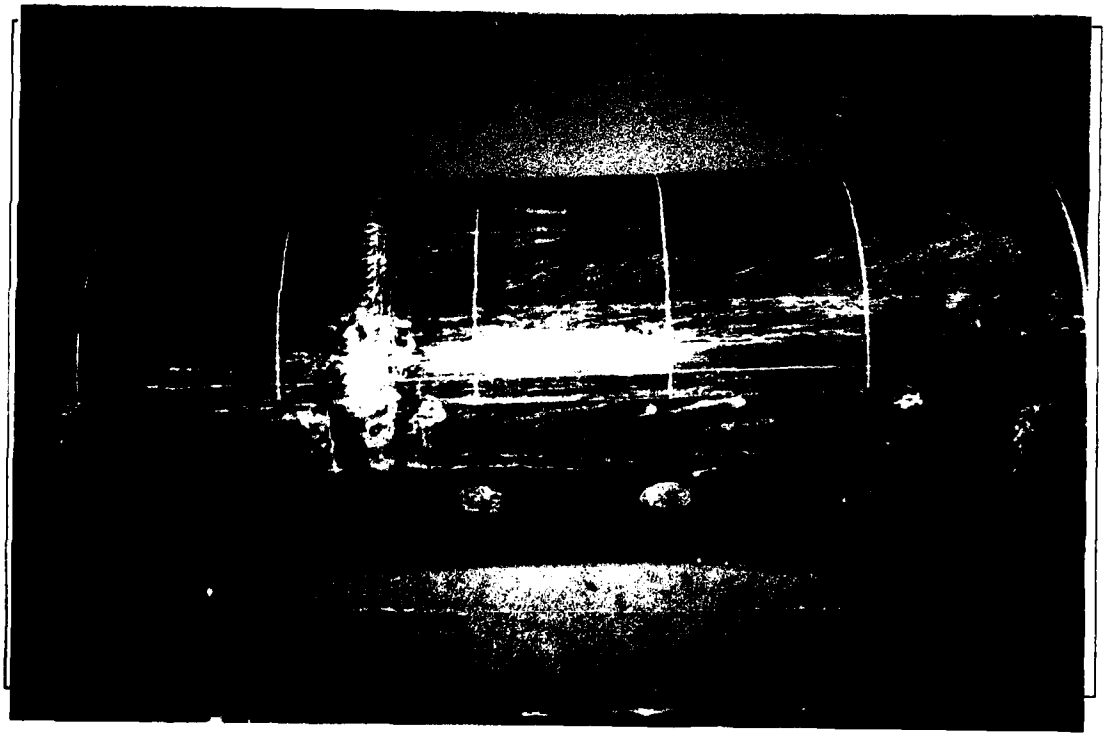

Figure A12. x = to x = 64".

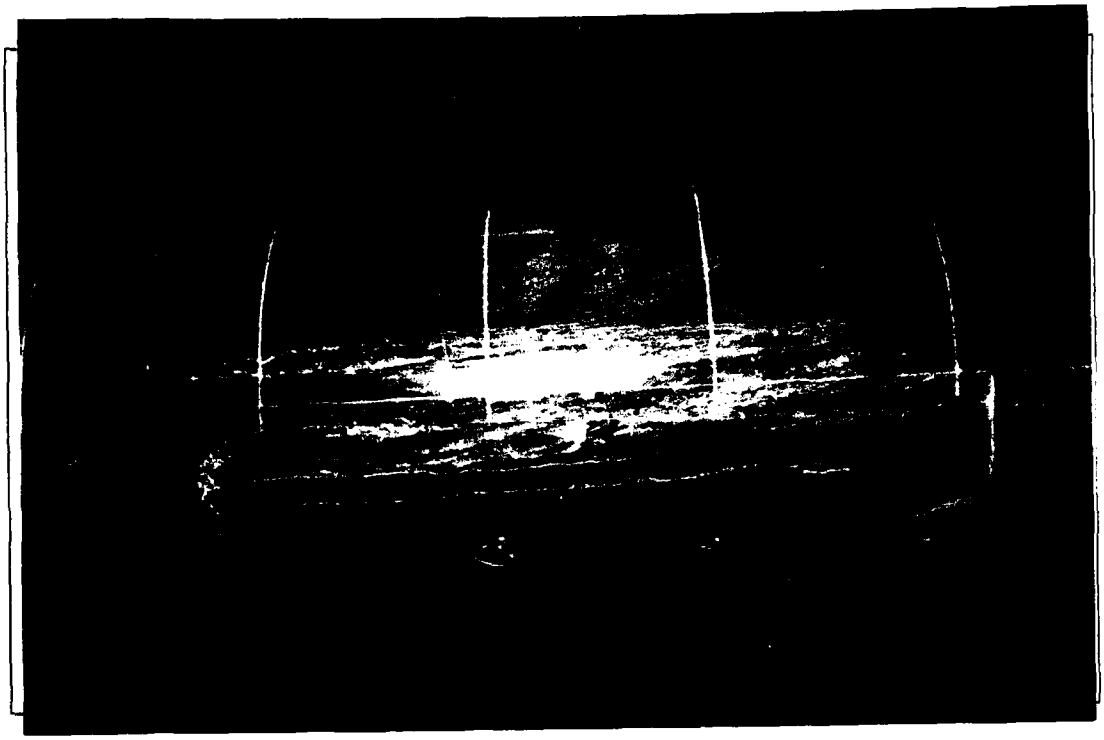

Figure A13 x = 32" to x = 48".

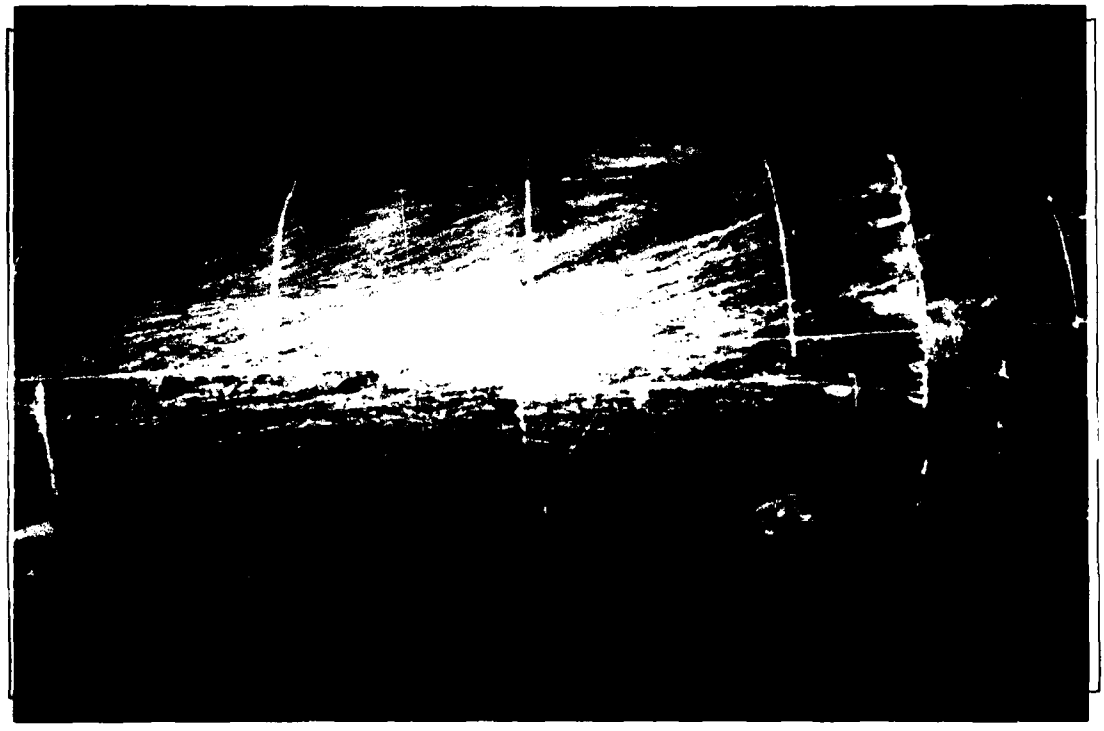

Figure A14. x = 16" to x = 32".

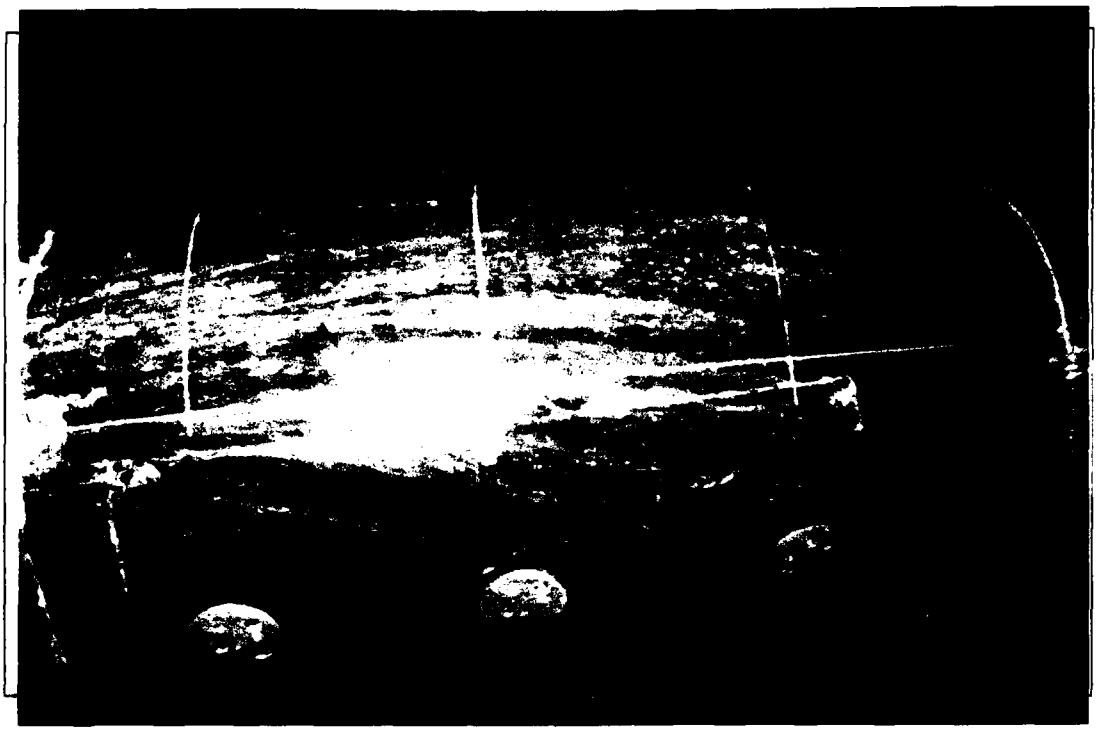

Figure A15. x = 4" to x = 16".

ß=15°, Bottom of Submarine.

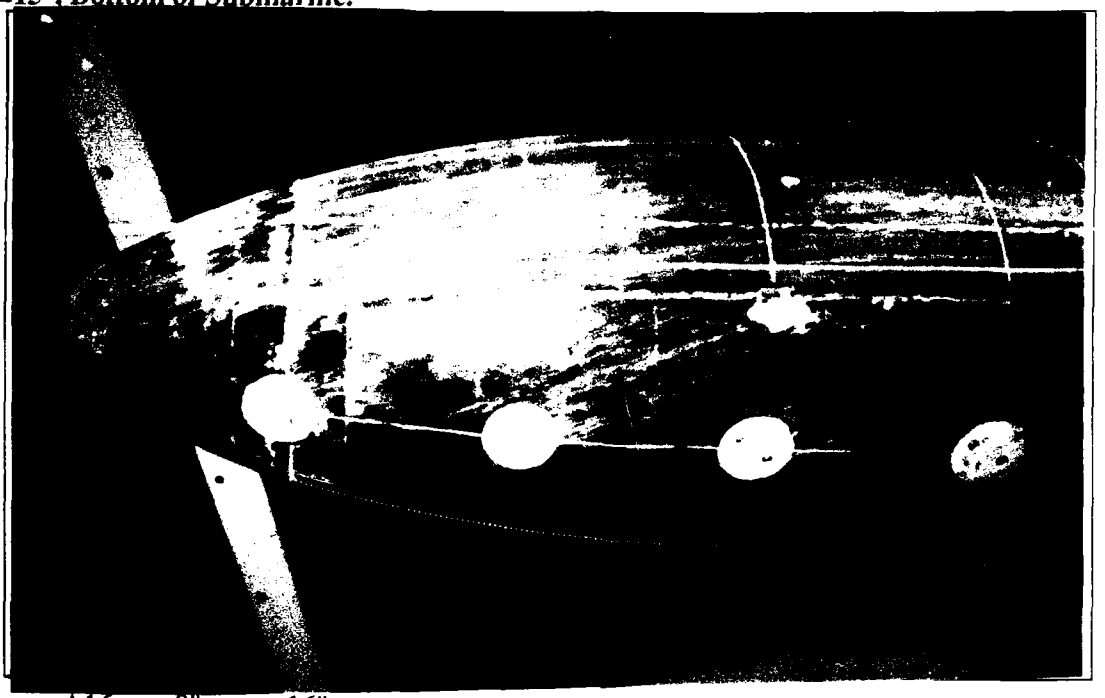

Figure A16. x = 0" to x = 16".

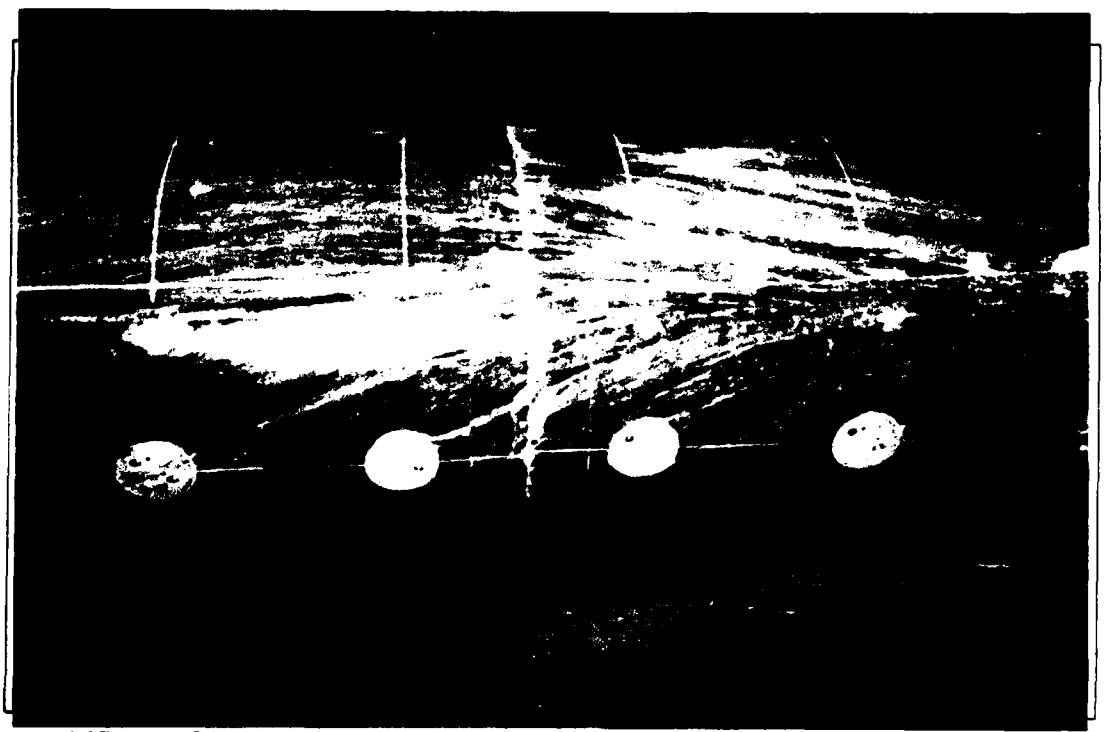

Figure A17. x = 12" to x = 28".

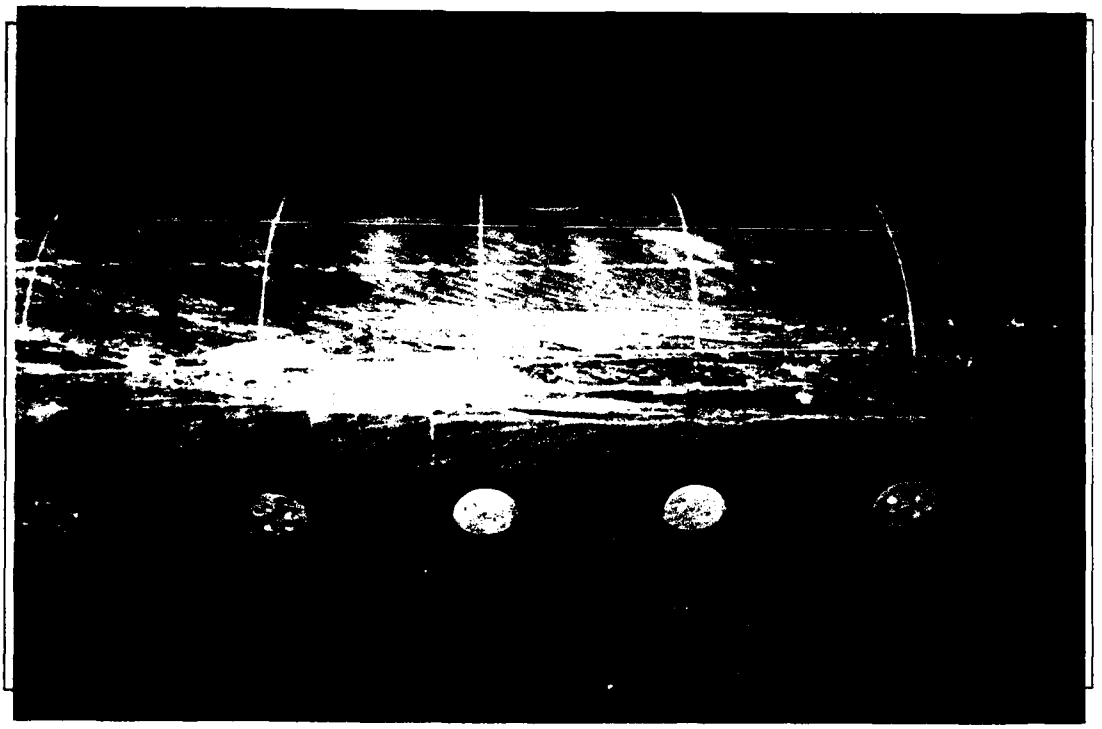

Figure A18. x = 24" to x = 44".

Figure A19. x = 40" to x = 60".

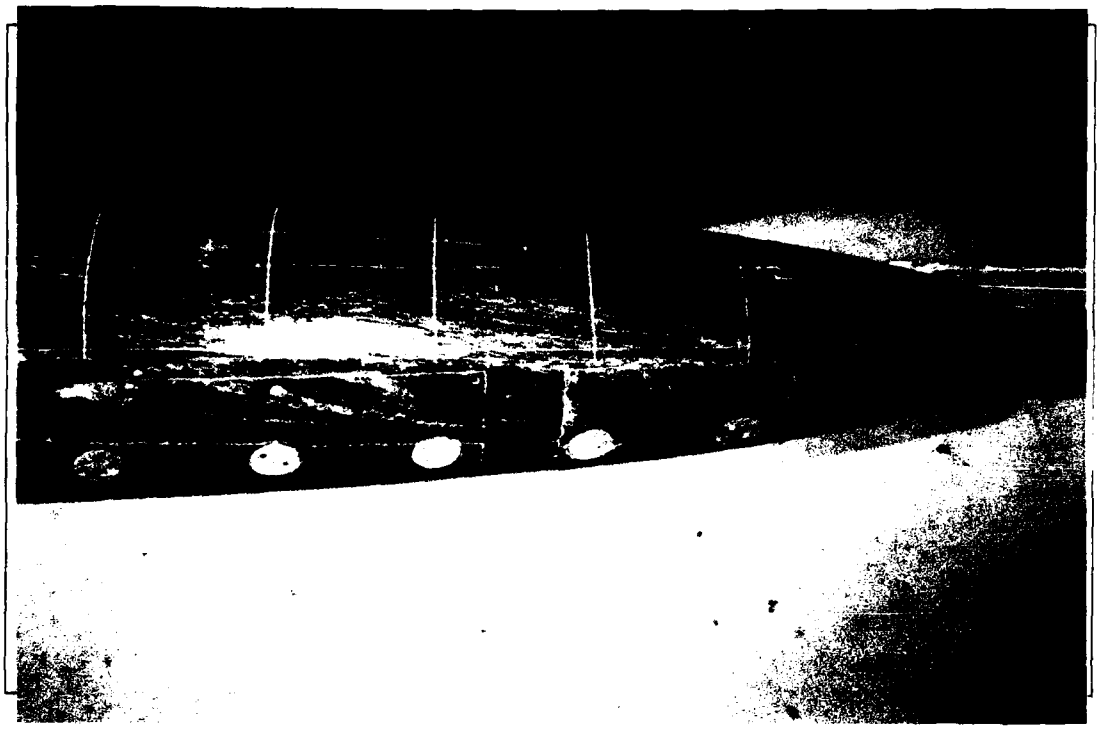

Figure A20. x = 60" to tail.

ß=10°, Top of Submarine (with towed array housing).

Figure A21. x = 60" to tail.

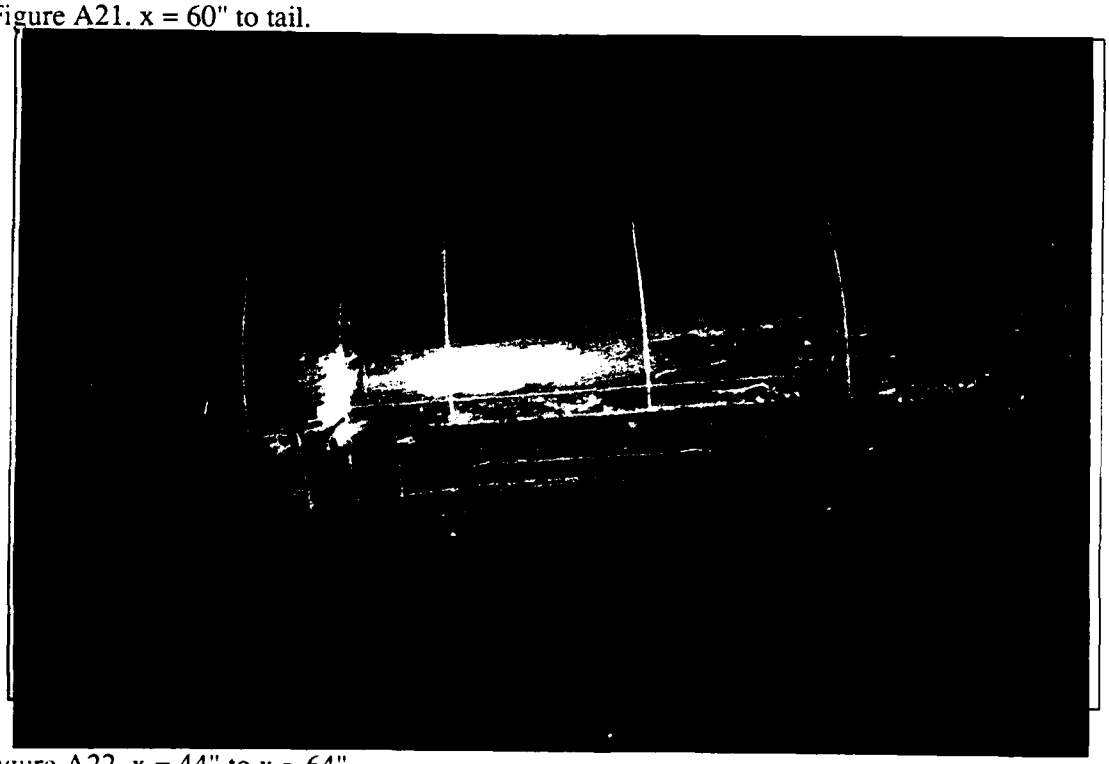

Figure A22. x = 44" to x = 64".

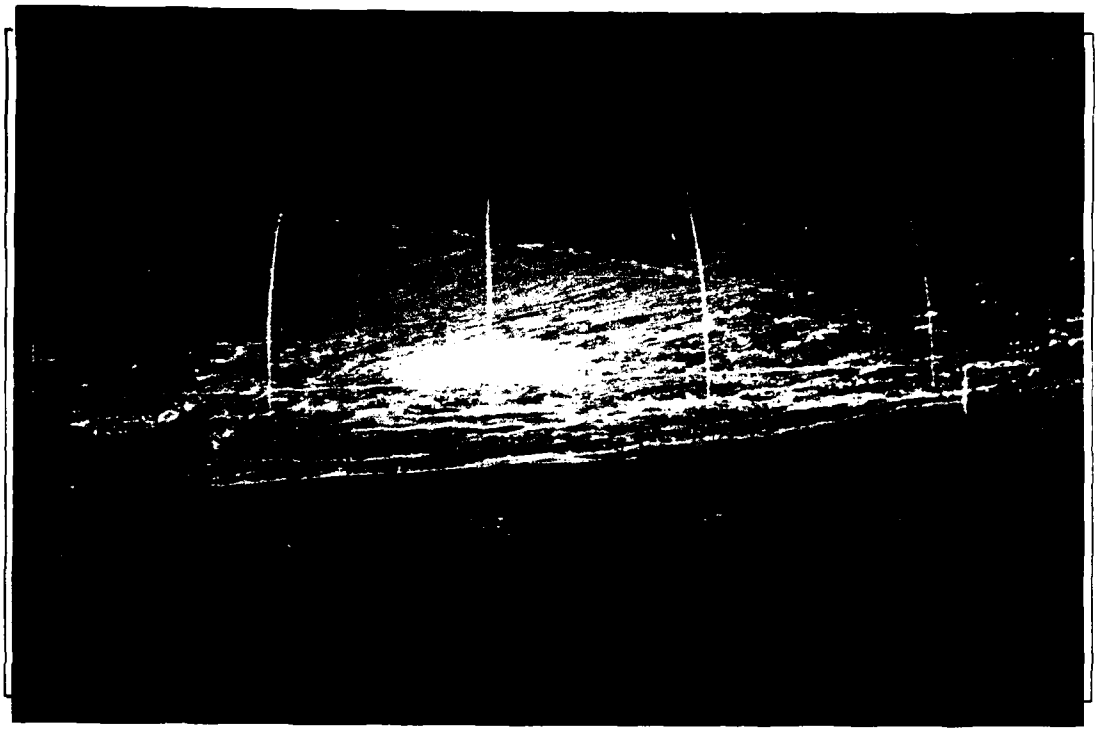

Figure A23. x = 32" to x = 48".

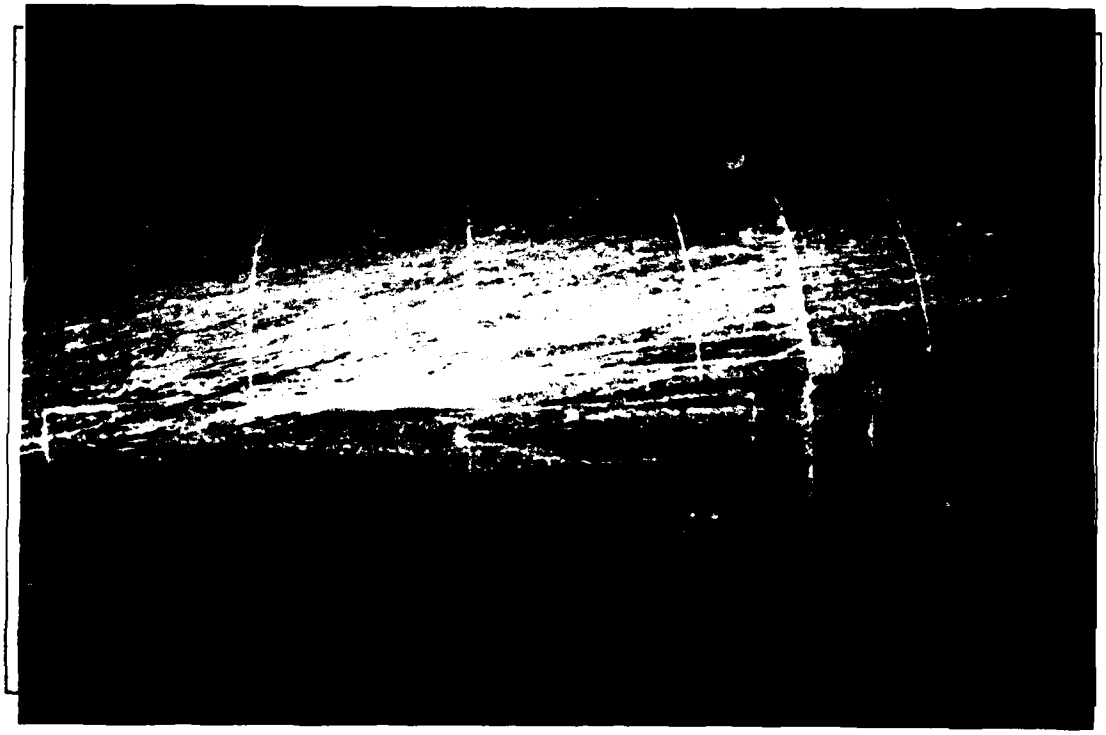

Figure A24. x = 16" to x = 32".

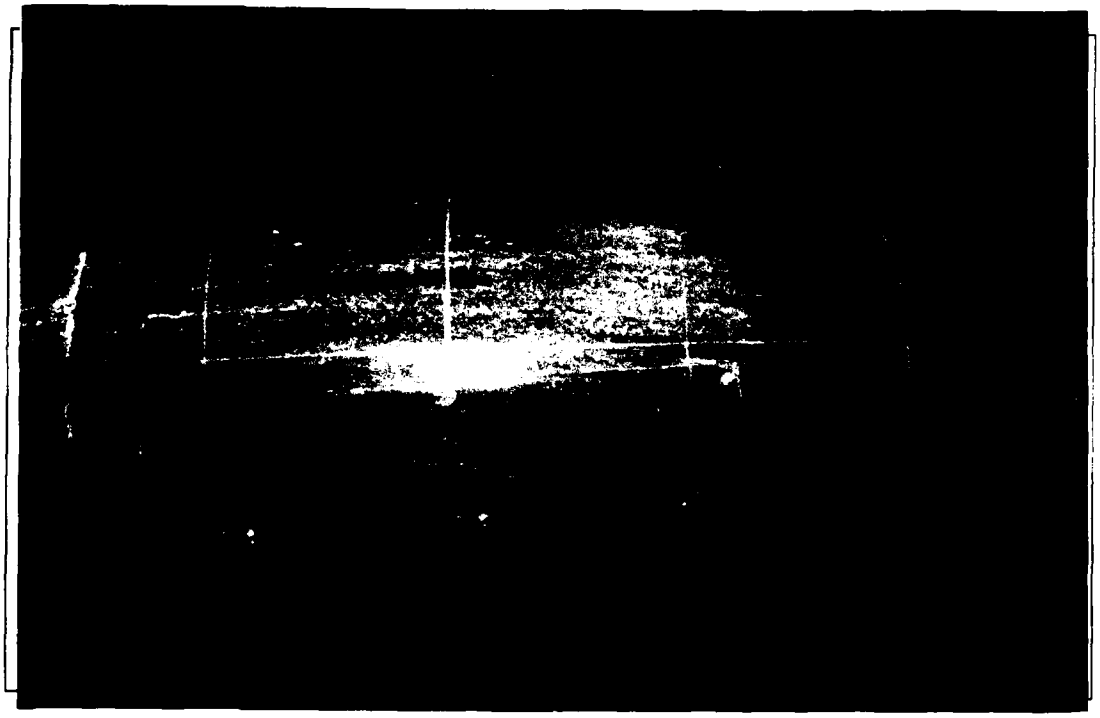

Figure A25. x = 0" to x = 16".

ß=10°, Bottom of Submarine.

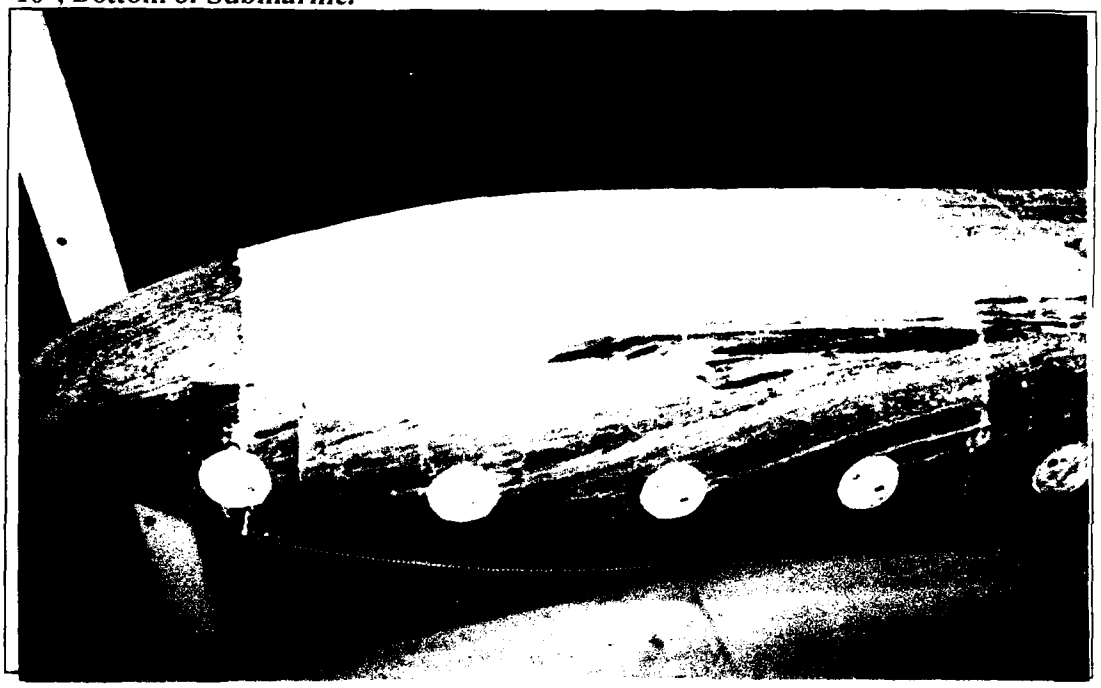

Figure A26. x = 0" to x = 20".

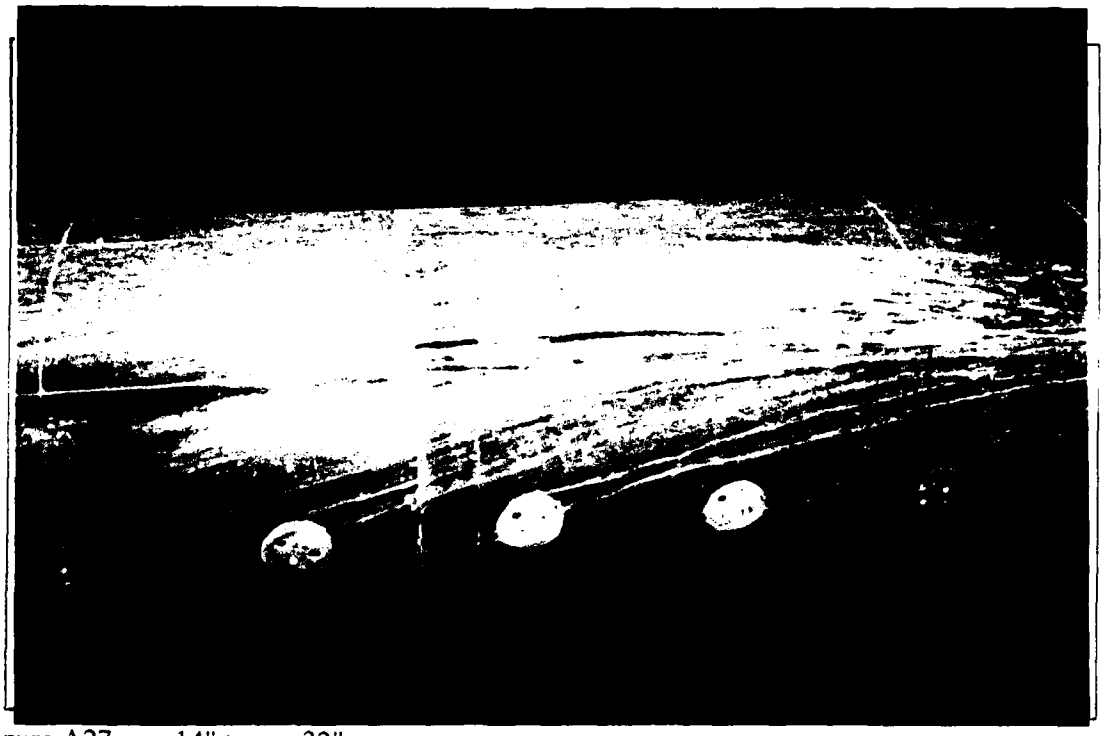

Figure A27. x = 14" to x = 32".

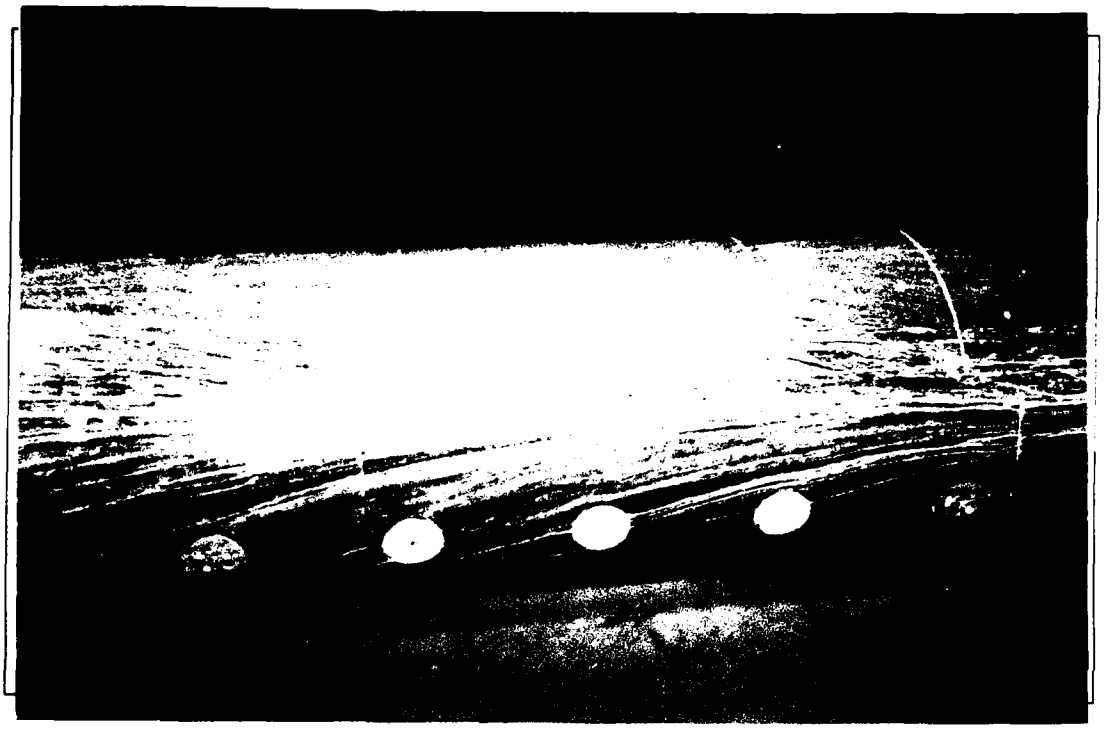

Figure A28. x = 28" to x = 48".

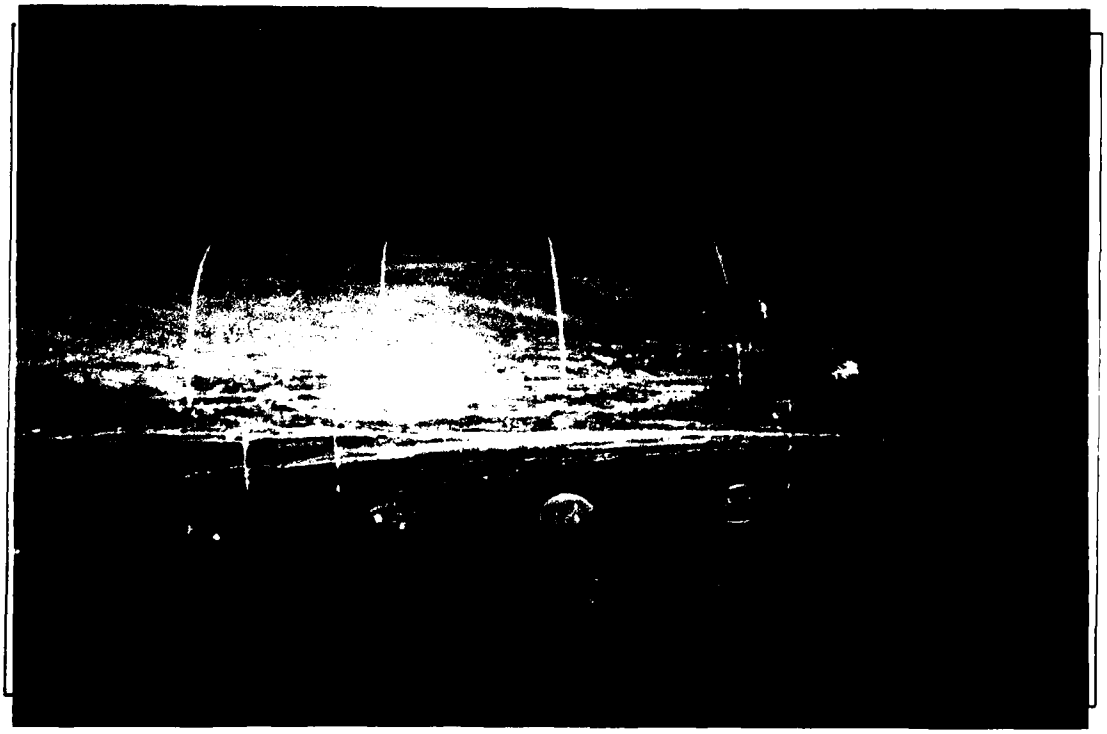

Figure A29. x = 44" to x = 64".

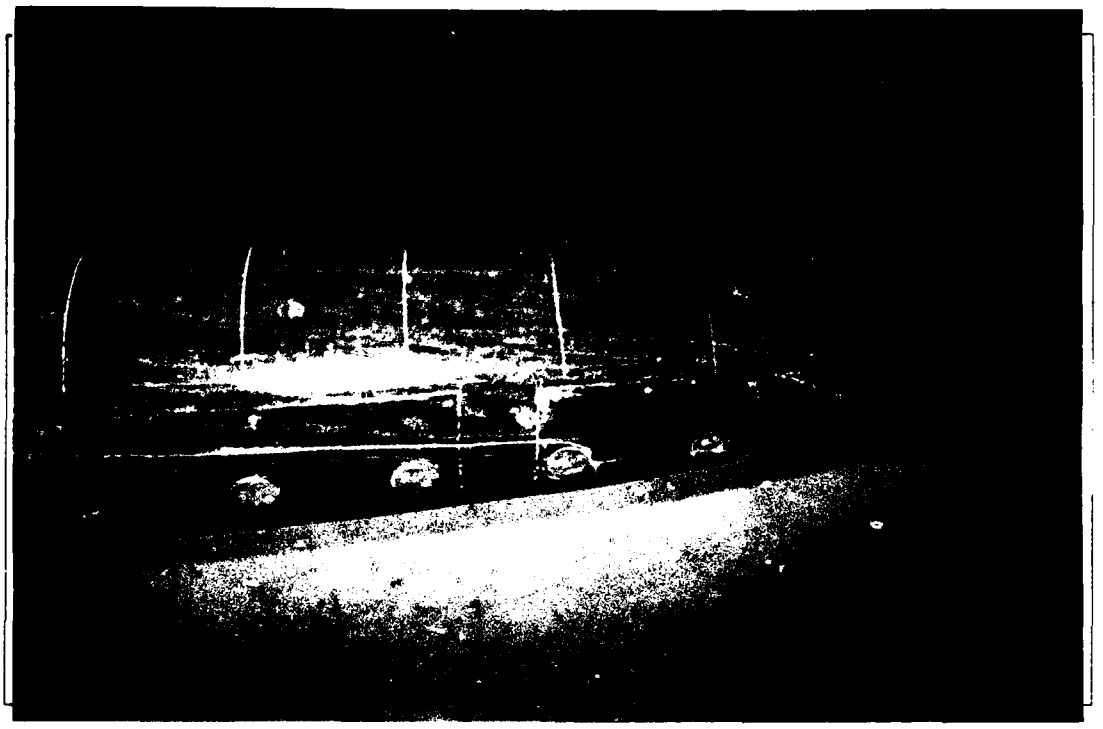

Figure A30. x = 60" to tail.

Appendix II - Model Offsets

The following table presents the actual shape data of the Model 1. The model diameters are given for the model at stations every four inches.

Body Dimensions: Los Angeles Class 688 Submarine Model

x, in.	x/c	Dh, in.	Dv, in.	Dh/c	Dv/c
4.00	0.044	5.68	5.61	0.0629	0.0621
8.00	0.089	7.49	7.48	0.0829	0.0828
12.00	0.133	8.12	8.11	0.0900	0.0898
16.00	0.177	8.22	8.23	0.0910	0.0911
20.00	0.222	8.22	8.22	0.0911	0.0910
24.00	0.266	8.23	8.22	0.0911	0.0911
28.00	0.310	8.27	-	0.0916	-
32.00	0.355	8.25	8.23	0.0914	0.0911
36.00	0.399	8.23	8.21	0.0912	0.0910
40.00	0.443	8.22	8.22	0.0910	0.0910
44.00	0.488	8.21	8.21	0.0910	0.0910
48.00	0.532	8.22	8.24	0.0911	0.0913
52.00	0.576	8.22	8.24	0.0911	0.0913
56.00	0.621	8.33	8.24	0.0922	0.0913
60.00	0.665	8.20	8.20	0.0909	0.0909
64.00	0.709	8.00	8.03	0.0886	0.0889
68.00	0.754	7.57	7.57	0.0839	0.0839
72.00	0.798	7.07	7.09	0.0783	0.0786
76.00	0.842	6.15	6.13	0.0681	0.0679
80.00	0.886	4.87	4.90	0.0540	0.0543

Submarine Model:	Nominally 90.25" long Nominally 8.25" wide and high
Towed Array Housing:	Nominally 1.25" Wide Start at x = 11.8" End at x = 80.0" Each end is semicircular in top view, and blended into body
Sail:	1.67" wide 4.29" high Leading edge at x = 24.6" Trailing edge at x = 33.1"
Manufacturer:	The Scale Shipyard 5866 Orange Ave. #3 Long Beach, CA 90805-4146 (213)-428-5027

Appendix III - Tail Geometry

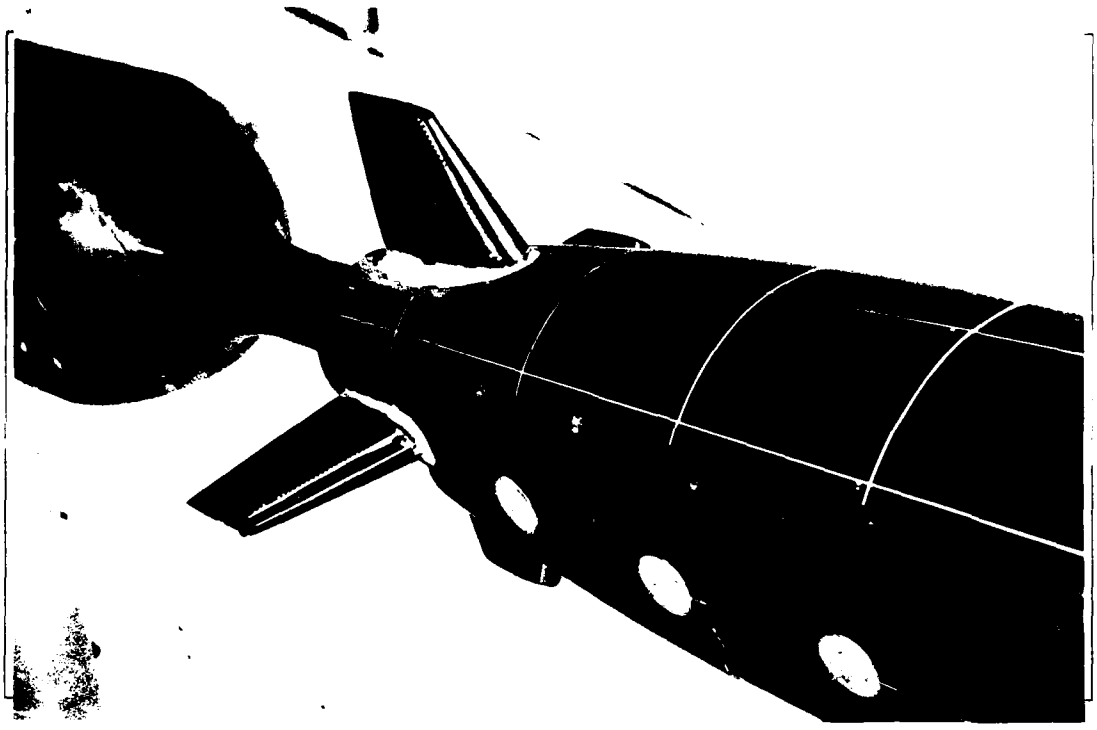

Figure A32. The trailing edge of all of the fins were placed at x=82". They were aligned relative to the model centerline to with +/-2° and were fixed for all studies. Given below is data describing the fin geometry. Coordinates are listed in tables describing the root airfoil shape. Figures are also provided giving fin planform dimensions. The root airfoil shape and thickness is scaled linearly from root to tip.

Vertical Fins

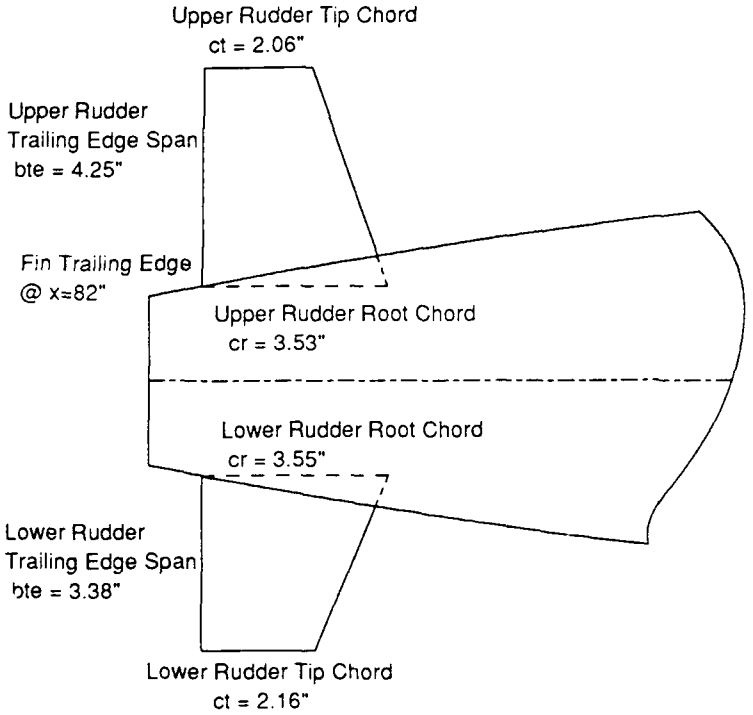

Lower Rudder Root Chord Dimensions

xr/cr	tr/cr/2
0.000	0.000
0.054	0.028
0.108	0.042
0.163	0.056
0.219	0.068
0.275	0.080
0.333	0.089
0.391	0.098
0.449	0.108
0.509	0.117
0.569	0.121
0.630	0.128
0.692	0.129
0.754	0.123
0.818	0.118
0.882	0.104
0.947	0.074

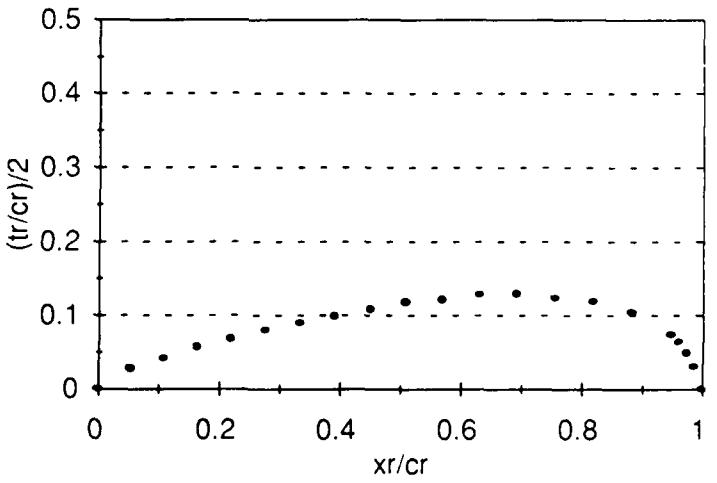

0.960	0.065
0.974	0.049
0.987	0.031
1.000	0.000

Upper Rudder

xr/cr	tr/cr/2
0.000	0.000
0.054	0.025
0.109	0.042
0.164	0.057
0.220	0.071
0.276	0.083
0.333	0.095
0.391	0.104
0.449	0.113
0.508	0.117
0.567	0.120
0.627	0.124
0.687	0.124
0.749	0.122
0.811	0.120
0.873	0.108
0.936	0.088
0.949	0.079
0.962	0.070
0.974	0.055
0.987	0.036
1.000	0.000

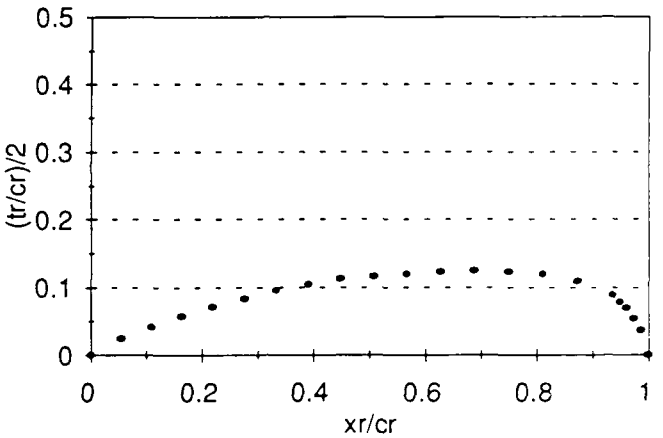

Horizontal Fins

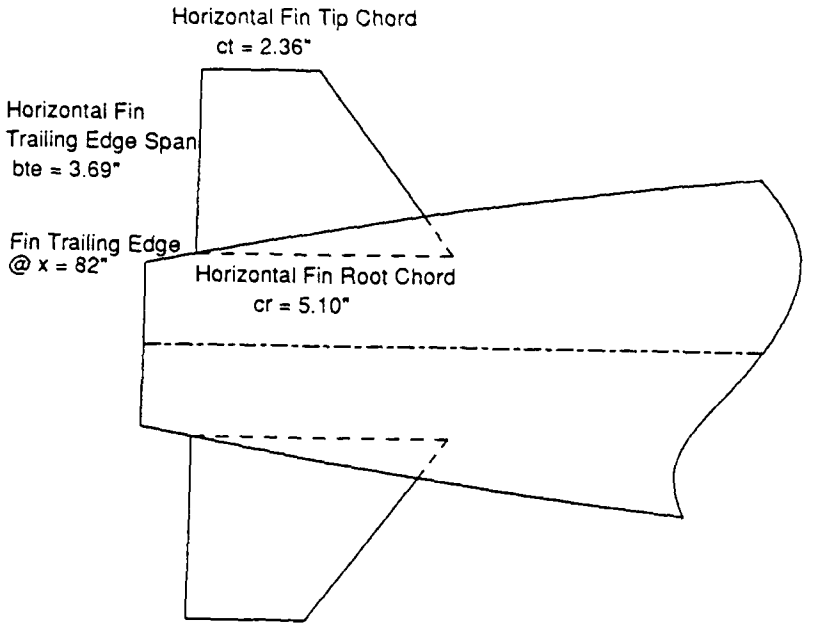

xr/cr	tr/cr/2
0.000	0.000
0.038	0.023
0.076	0.039
0.114	0.053
0.154	0.066
0.194	0.078
0.234	0.089
0.275	0.098
0.317	0.107
0.359	0.116
0.403	0.123
0.446	0.128
0.491	0.133
0.536	0.137
0.582	0.138
0.629	0.139
0.676	0.138
0.725	0.137
0.774	0.131
0.824	0.119
0.874	0.109
0.926	0.087

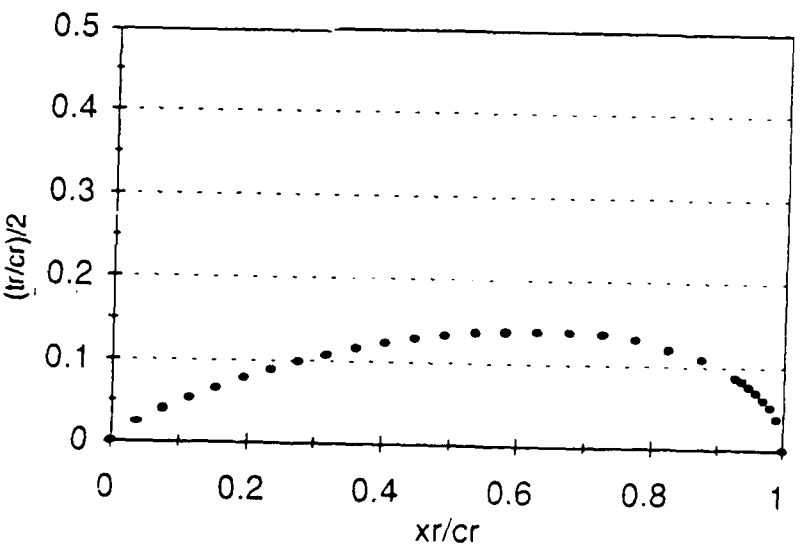

0.937	0.082
0.947	0.076
0.958	0.069
0.968	0.060
0.979	0.051
0.989	0.037
1.000	0.000

Sail Geometry

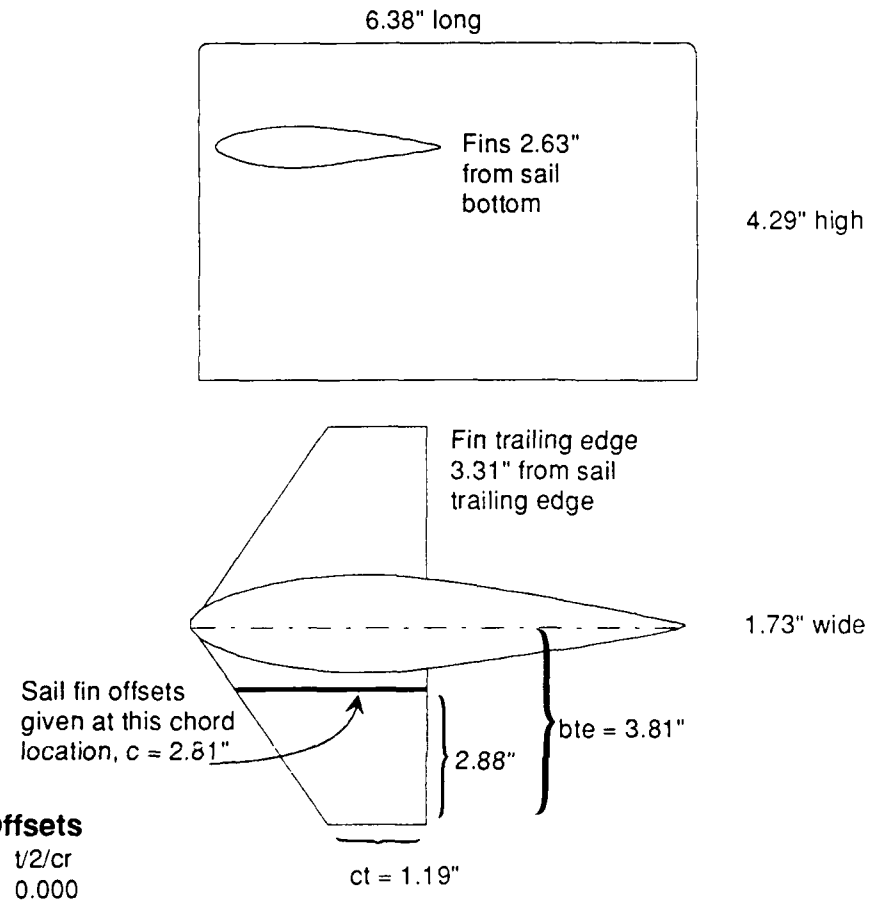

Sail Offsets

x/cr	t/2/cr
0.000	0.000
0.012	0.015
0.074	0.037
0.136	0.052
0.198	0.071
0.259	0.086
0.321	0.102
0.383	0.114
0.444	0.123
0.506	0.130
0.568	0.133
0.630	0.136
0.691	0.136
0.753	0.133
0.815	0.127
0.877	0.108
0.938	0.083
0.963	0.065
0.975	0.056
0.988	0.034
1.000	0.000

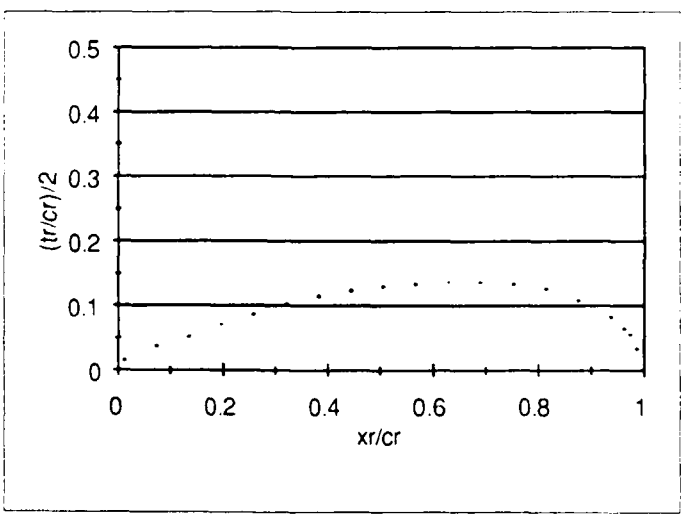

Sail Fin Offsets

x/cr	t/2/cr
0.000	0.000
0.054	0.034
0.122	0.061
0.189	0.074
0.257	0.095
0.324	0.108
0.392	0.115
0.459	0.122
0.527	0.128
0.595	0.135
0.662	0.135
0.730	0.128
0.797	0.122
0.865	0.108
0.932	0.081
0.973	0.054
0.986	0.027
1.000	0.000